

15th International Workshop for Young Scientists

BioPhys Spring 2016

BPS 2016

May 5-6, 2016 Prague, Czech Republic

BOOK OF ABSTRACTS



Czech University of Life Sciences
Prague, Czech Republic



Institute of Agrophysics, Polish Academy
of Sciences, Lublin, Poland



Polish Academy of Sciences
Branch in Lublin, Poland



Slovak University of Agriculture
Nitra, Slovak Republic



Szent István University, Gödöllő, Hungary



CZECH UNIVERSITY OF LIFE SCIENCES PRAGUE

Department of Physics

**15th International Workshop
for Young Scientists**

BioPhys Spring 2016

BPS 2016

BOOK OF ABSTRACTS

May 5-6, 2016

Prague, Czech Republic



PAN
POLSKA AKADEMIA NAUK
ODDZIAŁ W LUBLINIE



**INSTITUTE OF
AGROPHYSICS**
P A S



Edited by: Martin Libra and Jan Sedláček

Copyright© 2016 by Czech University of Life Sciences Prague,
Czech Republic

ISBN 978-83-89969-42-2

Edition: 100 copies
Printed by Perfekta info
www.perfekta.info.pl

CONTENTS

INTRODUCTION.....	5
SCIENTIFIC BOARD.....	6
LECTURES	7
<i>Abilzhanuly T., Abilzhanov D.T., Alshurina A.</i> : Effects of humidity variation on density and modulus of elasticity of wheat straw.....	8
<i>Askarbekov R.N., Duishenaliev T.B.</i> : The compression rubber-metal supports by using Cauchy tensor.....	10
<i>Baranowski P., Krzyszczak J., Sławiński C., Zubik M.</i> : Modelling climate change impact on crop production.....	12
<i>Bilińska-Wielgus N., Frąc M.</i> : The impact of heat treatment on metabolic profiles of fungi belong to <i>Neosartorya</i> genus.....	14
<i>Brunerová A., Brožek M.</i> : Influence of feedstock particle size on physical properties of solid biofuel from pine bark.....	16
<i>Gos M., Siedliska A., Zubik M., Jędryczka M., Baranowski P.</i> : Application of thermography and hyperspectral techniques for testing the resistance of tobacco (<i>Nicotiana Tabacum L.</i>) plants to the tobacco mosaic virus (TMV).....	18
<i>Hlaváč P., Božiková M.</i> : Effect of various factors on selected fermented wort rheologic properties.....	20
<i>Horabik J.</i> : Visco-elastic and elastic-plastic contact interactions of seeds during impacts.....	22
<i>Jaromin-Gleń K., Babko R., Kuzmina T., Łagód G., Bieganowski A.</i> : Periphyton Communities In Wastewater Treatment In Lublin (Poland) – Case Study.....	24
<i>Kabutey, A., Herák, D., Sigalingging, R., Divišová, M.</i> : Mechanical Behaviour and Loading Curves of Selected Bulk Oilseeds under Linear Compression.....	26
<i>Koczańska M., Cieśla J., Bieganowski A.</i> : The size and electrophoretic mobility of the biosurfactant aggregates at a different salt concentration.....	28
<i>Kouřím P., Libra M., Poulek V.</i> : Behavior of photovoltaic system during solar eclipse.....	30
<i>Kubík L.</i> : Compressive Properties of Pellets.....	32
<i>Lalak J., Kasprzycka A., Tys J.</i> : Effect of ultrasonic pretreatment on biogas production potential from <i>Agropyron elongatum</i> biomass.....	34
<i>Lešetický J.</i> : Methodology for testing the accuracy of GPS autonomous UAVs as perimeter protection.....	36
<i>Malínek M., Božiková M., Hlaváč P., Cviklovič V., Olejár M., Pavlovič S.</i> : Influence of temperature on power of photovoltaic modules.....	38
<i>Olšan T., Libra M., Poulek V., Avramov V.</i> : Experience Gathered with the unique Photovoltaic Power Plant in Central Part of Historical City.....	40
<i>Panek J., Frąc M.</i> : Loop-mediated isothermal amplification (LAMP) for detection of <i>Talaromyces flavus</i>	42
<i>Regrut T., Hlaváčová Z., Petrovič A., Csillag J.</i> : Electrical Properties of Perga.....	44
<i>Siecińska J., Nosalewicz A.</i> : The effect of supplementary red and blue light on the growth of lettuce under white fluorescent lamps.....	46

<i>Siedliska A., Baranowski P.:</i> Detection of gray mold infection using hyperspectral reflectance imaging	48
<i>Stelmach W., Shahbaz M., Bieganowski A., Kuzyakov Y.:</i> Sequestration of sludge C in soil as assessed by ¹³ C abundance and ¹⁴ C labelling	50
<i>Al-Neama M. A., Farkas I.:</i> Modelling of Solar Air Heater Integrated with Dryer Chamber ...	52
<i>Farkas I.:</i> Current Status of the use of Solar Thermal Energy	54
<i>Mészáros Cs., Nikolényi I., Bálint Á.:</i> Symmetry Analysis of Collective Elementary Excitations of Chain-type Organic Molecules, relevant for Solar Cells	56
<i>Seres I.:</i> Biophysical experiments on human senses	58
<i>Tóth J., Mészáros Cs., Bálint Á.:</i> Refinement of temperature data in soil column experiments	60
<i>Víg P.:</i> Physical properties of birch sap	62

INTRODUCTION

Dear Friends and Colleagues,

It is really my great pleasure to welcome you in attending the 15th International Workshop for Young Scientists "BioPhys Spring 2016" (BPS 2016) which, this time, going to be held in Prague, Czech Republic during May 5-6, 2016. The meeting continues the tradition of previous workshops oriented on training of young researchers and exchange of professional experience in the field of physics applied to biological, agricultural and food systems as well.

It is cordially invited the young scientists to participate in the activity of BPS 2016 Workshop, and to present their results of research in application of physics to life sciences. The Workshop is organized as an opened English spoken event without registration fee.

Two-page abstracts of contributions are published in an ISBN numbered printed BPS Book of Abstracts.

It is my pleasure to invite you to spend a few days of May 2016 in friendly atmosphere between young people in Prague.

During your stay, you may visit the facilities of the Czech University of Life Sciences Prague, the laboratories and installations of the Faculty of Engineering, especially Department of Physics and of course, the city of Prague and its area.

Special thanks are devoted to the Faculty of Engineering, Czech University of Life Sciences Prague, Czech Republic for the support of organizing the event of BPS 2016.

Prof. Martin Libra

Chairman, BPS 2016

SCIENTIFIC BOARD

Prof. RNDr. Ing. Jiří Blahovec, DrSc.	Czech University of Life Sciences Prague, Czech Republic
Prof. Dr. István Farkas	Szent István University, Gödöllő, Hungary
Prof. Dr. hab. Jan Glinski	President of the Lublin Branch of Polish Academy of Sciences, Lublin, Poland
Ass. Prof. RNDr. Zuzana Hlaváčová, CSc.	Slovak University of Agriculture, Nitra, Slovak Republic
Prof. Dr. hab. Józef Horabik	Institute of Agrophysics Polish Academy of Sciences, Lublin, Poland
Prof. Ing. Martin Libra, CSc.	Czech University of Life Sciences Prague, Czech Republic
Ass. Prof. Dr. István Seres	Szent István University, Gödöllő, Hungary
Ass. Prof. RNDr. Vlasta Vozárová, Ph.D.	Slovak University of Agriculture, Nitra, Slovak Republic

LECTURES

Effects of humidity variation on density and modulus of elasticity of wheat straw

Abilzhanuly T. ¹. Abilzhanov D.T. ¹. Alshurina A. ²

¹ Kazakh Scientific Research Institute of Mechanization and Electrification of Agriculture.
Rayimbek avenue. 312. 050010 Almaty. Republic of Kazakhstan

² Czech University of Life Sciences Prague. Kamýcká 129. 16521 Prague 6. Czech Republic

Corresponding author: Alshurina A.. e-mail: alshurina@inbox.ru

Keywords: modulus of elasticity, moisture content, density of the material st.

Results of previous studies [1] have shown that at the same humidity the lowest elastic modulus value of all types of roughage have stems of barley straw. It is known that with an increase in the value of the elastic modulus of the material destruction occurs at low energy consumption. At the same humidity straw stalk crops destroyed worse in comparison with other types of stems roughage (e.g.. Agropyron, Alfalfa). Therefore, for experimental research on working bodies of feeding units were chosen stems of wheat straw.

The density of the material stems in a large extent depends on the humidity. In variation of humidity of barley straw from 0 to 35% its density are within [1]: $p = 125...200 \text{ kg/m}^3$, $p_m = 300...470 \text{ kg/m}^3$. Determination of bulk density and density of the material stems was carried out during the experiment on research of the elastic modulus as a function of stems moisture content.

For the experiment were chosen 9 stems of wheat straw which were divided into three groups. The diameters of the stems in each group ranged 3.05...3.25mm and 4.06...4.21 mm. and their inside diameters are respectively equal 1.65...1.7 mm and 3.1... 3.25 mm. (see Tab. 1).

Tab. 1 The initial indicators of stems of wheat straw.

№ of stems	L_{st} , mm	The average outer diameter of the stem, mm	The average inner diameter of the stem, mm
1.	425	4.06	3.10
2.	376	4.21	3.25
3.	329	4.15	3.20
4.	380	3.25	2.45
5.	350	3.11	2.40
6.	240	3.05	2.35
7.	298	2.10	1.70
8.	296	2.08	1.65
9.	160	2.10	1.70

To change the moisture content at first stems saturated with moisture and stored in a plastic bag 48 hours. In the experiment to determine the elastic modulus and the density of stems, changes in a moisture level is achieved by drying stems at room temperature.

To determine the mass of stems used weighing scales. Determination of the natural frequency of stems investigated in a setup consisting of filmscope, oscilloscope H-700, photo resistor CSF-1 and tested stem, the butt of a cantilever embedded in a wooden clamp [2].

Thin light beam directed to the photo resistor through the console is embedded stem. Stalk in rest state blocked the way of the light flux to the photo resistor. When free oscillations cantilever embedded in a wooden clamp stems, changing the amount of light falling on the surface of the photo resistor, which changes the electrical resistance of the latter. This signal is

fed via an amplifier to an oscilloscope. According to oscillogram by a known period of oscillations determined the natural frequencies of stems.

Knowing the frequency of natural oscillations of stems, their elastic modulus was calculated using the known formula [2]:

$$E_{st} = \frac{F_{st} \rho_m L_{st}^4 f_{st}^2}{0,313 J_{st}}$$

where F_{st} – cross-section of the stem, m²;

ρ_m – stems material density, kg/m³;

L_{st} – stems length, m;

f_{st} – natural frequency, Hz;

J_{st} – moment of inertia of the stem cross-section, m.

The values of the modulus of elasticity, bulk density and the density of the material stems

were determined by the average values of investigated 9 stems. During the experiment, stem density was determined by taking into account their volume, calculated on the outside diameter, and the density of the material stems was determined taking into account the volume occupied by the material only, i.e. stem volume was calculated without considering their internal volume.

Variation of density of the wheat straw stems shows that, by increasing the moisture content increases its value. At the same humidity, density of material stems two times more than the density of stems.

Regularity of variation modulus of elasticity in wheat stalks shows that up to 30% moisture content its values dramatically changed, a further increasing of humidity is decreased of the intensity. Thus, we can assume that stems have elastic properties up to 30% moisture content, as a further increasing the moisture content their elastic properties almost not changed.

References

- [1] Abilzhanov T. Research and a substantiation of parametres of working organs chopper roughage hammer type. Journal Agro Engineering, 2001, №2, pp.12-15.
- [2] Abilzhanov T. Feed processing plant for agricultural farms: training book. Astana, 2007, 200p.
- [3] Landau L.D., Lifshitz E.M. The theory of elasticity. - Moscow.: Nauka, 1965.203 p.

The compression rubber-metal supports by using Cauchy tensor

Askarbekov R.N.¹, Duishenaliev T.B.²

¹ Czech University of Life Sciences Prague, Kamýcká 129, 16521 Prague 6, Czech Republic

² Kyrgyz State Technical University, Mira 66, 720044 Bishkek, Kyrgyz Republic

Corresponding author: Askarbekov R.N., e-mail: askarbekov@tf.czu.cz

Keywords: rubber metal, Matlab, Cauchy tensor

Abstract

We use Cauchy tensor for calculating stress-strain state of rubber metal supports, and we define the deformation by the displacement of every point in the volume. The investigated material area of the body with a volume V have an acting external forces, which denote as f_i . The external forces acting on the surface - S of this volume, denoted by p_i . Further we written in the classical form of the condition of equilibrium of the body volume under the action of these forces it [4].

$$\begin{aligned}\sigma_{ji,j} + f_i &= 0, \quad \sigma_{ij} = \sigma_{ji}, \quad x_i \in V \\ \sigma_{ij,kk} + \frac{1}{1+\nu}\sigma_{kk,ij} + \frac{\nu}{1-\nu}\delta_{ij}f_{k,k} + f_{i,j} + f_{j,i} &= 0, \quad x_i \in V \\ \sigma_{ji}n_j &= p_i, \quad x_i \in S\end{aligned}$$

where ν the Poisson's ratio

Follows from the solution of the static boundary problem are determined the deformation

$$\varepsilon_{ij} = \frac{1}{E}(-\nu \cdot \delta_{ij} \cdot \sigma_{kk} + (1+\nu)\sigma_{ij})$$

where E is Young's modulus.

Next, we determine the displacement $u_i(x)$ by the Cesàro formulas

$$u_i(x) = \frac{1}{E} \int c \left(-\nu \delta_{ik} x_3 + (1+\nu) \delta_{i2} \delta_{k2} x_3 + (x_j - y_j) \left(-\nu (\delta_{ki} \delta_{3j} - \delta_{kj} \delta_{3i}) + (1+\nu) \delta_{k2} (\delta_{i2} \delta_{3j} - \delta_{j2} \delta_{3i}) \right) \right) dy_k, \quad x_i \in V$$

Integrating this expression, we find

$$\begin{aligned}u_1(x) &= -\frac{c \nu x_3 (x_1 - x_1^0)}{E}, \quad x_i \in V \quad \text{and} \quad u_2(x) = \frac{c x_3 (x_2 - x_2^0)}{E}, \quad x_i \in V \\ u_3(x) &= -c \left(\left(x_2^2 + \nu (x_3^2 + x_1^2) - x_2^0 (2x_2 - x_2^0) - \nu \left((x_3^0)^2 - x_1^0 (2x_1 - x_1^0) \right) \right) / 2E \right), \quad x_i \in V\end{aligned}$$

The function is satisfying the equilibrium equations in the Navies form [4]. Finally, from a field of displacement we define the components of deformation and rotation

$$\begin{aligned}\varepsilon_{ij} &= c x_3 \left(-\nu (\delta_{i1} \delta_{j1} + \delta_{i3} \delta_{j3}) + \delta_{i2} \delta_{j2} \right) / E, \quad x_i \in V \\ \omega_{ij} &= -c \left(\nu (x_1 - x_1^0) (\delta_{1i} \delta_{3j} - \delta_{3i} \delta_{1j}) - (x_2 - x_2^0) (\delta_{2i} \delta_{3j} - \delta_{3i} \delta_{2j}) \right) / E, \quad x_i \in V\end{aligned}$$

According to the obtained expressions we can determine stress components, deformation and rotation anywhere in equilibrium in body V .

Figure 1, shown on the left, the compression rubber metal supports under the press and the right compression model in Matlab system. To solve this problem of elasticity theory custom code was written in Matlab. According to this code, this body can be divided into thousands of points and to determine the movement of each point by the action of compressive forces on it. For more information to how to use this method are obtained in reference [3]. According to the obtained equations of motion of points is constructed of rubber metal support when exposed to compressive force.

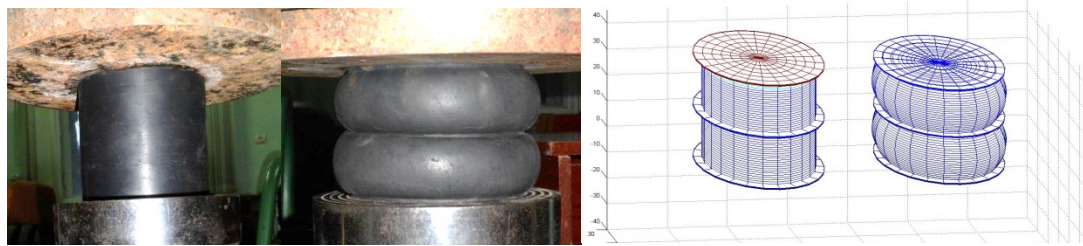


Fig. 1 Under uniform load the compression of rubber-metal supports.

Figure 2 shows the compression rubber metal supports for different values of compressive forces. The supports of such form are used to protect machines and equipment from the vibrations. Be used a special amortization rubber for the manufacture of such supports. In these constructions is deformed only rubber layers under compression [5].

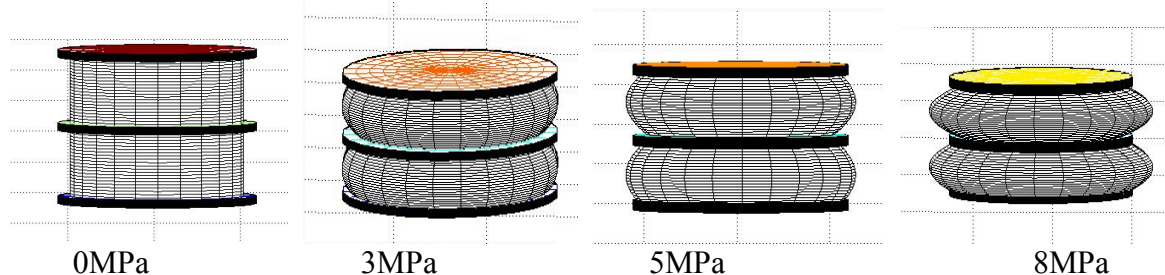


Fig. 2 The deformation process under different values of the load, which is applied on top.

For a description of deformation of the rubber layer is usually used in the classical static boundary problem, the non-linearity of this material. Rubber is an anisotropic material and to describe the deformation by using classical mechanics expressions are not possible. In this paper we present a new method for determining the deformation by using Cauchy tensor [1, 2]. Deformation is determined by the displacement of points of the body, eliminating the consideration of many simplifications in the solution of this problem with the use of known expressions.

The implementation of this method by using Matlab allows you to visually see the results of calculations for each point and build on the movement of these points in Matlab volumetric three-dimensional body; all results are shown on the Figure 2.

Acknowledgement

The work was supported in Czech University of Life Sciences Prague by the CASIA project <http://www.eu-casia.org/home>. The authors thank for supporting all CASIA team.

References

- [1] Askabekov R.N. Construction of mathematical model, compression of rubber-metal supports and behavior of rubber layer. *Computational technologies*, Novosibirsk, 2015, 20, pp. 40-46
- [2] Askarbekov R.N. Modeling in ANSYS the compression of rubber-metal elements. *Mechanical Engineering*. Moscow, 2015, 4 (96), pp. 40-42.
- [3] Zhakypbek A.B., Duishenaliev T.B. *Mechanics of rigid body, new view on some basics*. Bishkek, 1999, 120 pages.
- [4] Nowacki W. *Theory of Elasticity*. Moscow, 1975, 872 pages.
- [5] Ormonbekov T. *The application of thin-layer rubber-metal elements for the seismo protection of buildings, structures and engineering equipment*. Bishkek, 1996, 25 pages.

Modelling climate change impact on crop production

Baranowski P., Krzyszczak J., Sławiński C., Zubik M.

Institute of Agrophysics Polish Academy of Sciences, Doświadczalna 4, 20-290 Lublin, Poland

Corresponding author: Baranowski P., e-mail: pbaranow@ipan.lublin.pl

Keywords: climate change, multifractality of meteorological time series, wheat yield, impact response surface

Abstract

The improved understanding of how climate change impacts crop yields is a research priority in the context of planning global food production and undertaking adaptation and mitigation measures [3]. The most effective way of predicting crop yield responses to climate change is the use of process-based crop models, which can contain various approaches for structuring and parameterization of the fundamental processes responsible for crop development and growth [2]. A combination of factors influence the actual and future crop yields including meteorological parameters (precipitation, air temperature, solar radiation, CO₂ concentration), soil parameters (soil texture and structure, water properties, organic matter, fertilization) and the occurrence of biotic and abiotic stresses [4]. The impact response surfaces are a convenient way of presenting the modelled sensitivity of various crop production quantities to changes in different climate variables. They are constructed by conducting multiple model simulations taking into account a wide range of probable future climate conditions as well as for the present-day conditions, and then plotting the estimated impacts against key climate variables [5]. In the temperate climate zones the studies of trends in average air temperature, or average precipitation are not sufficient to understand the processes occurring in the atmosphere and the consequences of these changes for living organisms. Therefore, it is necessary to look for more sophisticated methods of analysis of long-term meteorological series to be able to determine the long-range correlations, which can also be associated with climate change. Such methods are multifractal analysis and chaos theory, which help to determine the parameters easily linked to the dynamics of processes in the atmosphere being responsible for climate change [1].

The aim of this study was to develop mathematical and physical methods describing the state of the environment of plant growth taking into account climate change by using the multifractal analysis to describe the long-range correlations in agro-meteorological time series and by modelling, the impact of various scenarios of climate change and adaptation measures on grain yield.

Crop model simulations with the use of DNDC and WOFOST models were conducted for the Spanish location, Lleida, for winter wheat. The period 1981-2010 was used as the baseline. Three levels of CO₂ were simulated, and the adaptation measures were restricted to changes in sowing dates, cultivar phenology and supplementary irrigation. The results indicated high sensitivity of DNDC and WOFOST models to changes in CO₂ concentration in the atmosphere and to all the studied adaptation measures. An example of DNDC simulations of dry grain matter (DGM) for varying sowing days and watering conditions is presented in Fig. 1. The shapes of impact response surfaces (IRS) lines and the ranges of obtained DGM values for presented simulations varied considerably. The comparison of the IRS results for DNDC and WOFOST models indicated differences in isolines shape and direction which can be attributed to different model construction. The proposed approach shows consequences of climate change and chosen adaptation measures on wheat production. It is expected that the ensemble simulations being conducted in MACSUR project will deliver further reliable projections of crop production under climate change.

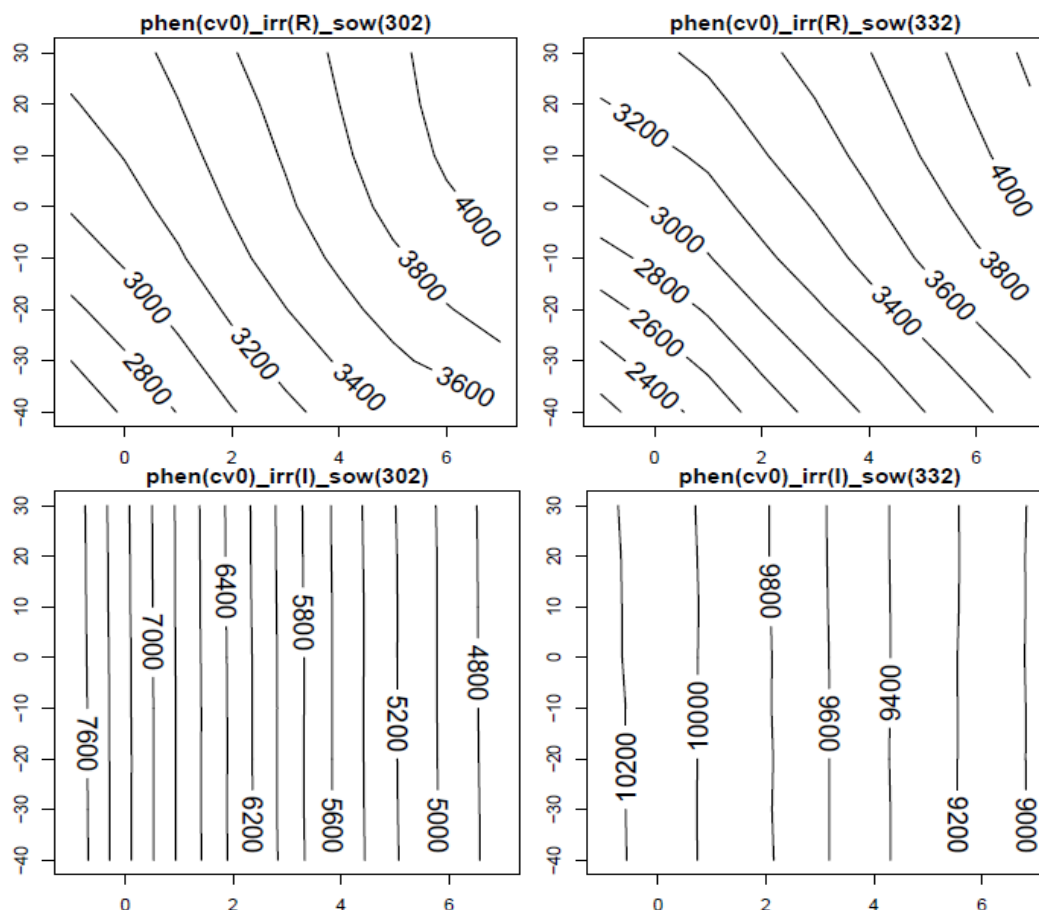


Fig. 1 An example of DND model impact response surfaces for chosen adaptation measures: two sowing days (302 and 332) and two water managements (rainfed conditions (R) and full irrigation conditions (I)).

Acknowledgement

This study was conducted in the context of CROPM, the crop modelling component of MACSUR (Modelling European Agriculture with Climate Change for Food Security), a project launched by the Joint Research Programming Initiative (JPI) on Agriculture, Food Security and Climate Change (FACCE) and has been partly financed from the funds of the Polish National Centre for Research and Development in frame of the project: LCAgri, contract number: BIOSTRATEG1/271322/3/NCBR/2015.

References

- [1] Baranowski P., Krzyszczak J., Sławiński C. et al., *Climate Research*, 2015, 65, pp. 39-52.
- [2] Challinor A.J., Watson J., Lobell D.B., Howden S.M., Smith D.R., Chhetri N., A meta-analysis of crop yield under climate change and adaptation. *Nat. Clim. Change*, 2014, 4: pp. 287–291.
- [3] Hertel T.W., Burke M.B., Lobell D.B., The poverty implications of climate-induced crop yield changes by 2030. *Global Environ. Change*, 2010, 20, pp.577–585.
- [4] Neumann K., Verburg P.H., Stehfest E., Müller C., The yield gap of global grain production: a spatial analysis. *Agric. Syst.*, 2010, 103, pp. 316–326.
- [5] Pirtioja N. et al., A crop model ensemble analysis of temperature and precipitation effects on wheat yield across a European transect using impact response surfaces. *Climate Research*, 2015, 65, pp.87–105.

The impact of heat treatment on metabolic profiles of fungi belong to *Neosartorya* genus

Bilińska-Wielgus N., Frać M.

Institute of Agrophysics Polish Academy of Sciences, Doświadczalna 4, 20-290 Lublin, Poland

Corresponding author: Bilińska-Wielgus N., e-mail: n.bilinska@ipan.lublin.pl

Keywords: *Neosartorya*, Biolog, FF Plates, catabolic profile

Abstract

The fungi of *Neosartorya* genus belong to phylum *Ascomycota* which is ubiquitous in soil throughout the world and they are involved in the spoilage of thermally processed fruit products. This fungi can grow even under reduced oxygen conditions. Moreover *Neosartorya* has been known to produce mycotoxins which can cause humans health problems [2]. *Neosartorya* is able to sexual reproduction involving the formation fruits bodies named cleistothecia. Cleistothecia contain asci with ascospores. Nevertheless, ascospores are main vehicle for dispersion mainly via air and water [1,2]. Ascospores of *Neosartorya* have been reported to be resistant against desiccation, high pressure and heating [4]. They are able to survive pasteurization treatments and even temperatures above 85°C even for 100 min [4]. They are considered to be the most stress-resistant eukaryotic cells [3,4]. The pasteurization treatment can even break the dormancy of the ascospores leading to germination [4]. The major solutes in fungal cells are sugar trehalose and polyols glycerol, erythritol, arabitol and mannitol. These molecules are compatible with cellular functioning even when present at high concentration. Stress-resistant ascospores contain large amounts of trehalose, trehalose-based oligosaccharides and mannitol [4].

The aim of the study was to evaluate the metabolic pattern of seven strains of *Neosartorya* (Tab. 1.) after heat shock (80°C, 30 min) under aerobic conditions (21% O₂) and microaerophilic conditions (6% O₂). Metabolic profile was evaluated using FF microplates (BiologTM). We obtained data on utilization of 95 carbon sources from different groups: carbohydrates, amino acids, amines and amides, polymers, carboxylic acids and miscellaneous substrates. Optical density (OD) was measured at 750nm wavelength. Metabolic profile was expressed as average well-colour development (AWCD).

Tab. 1 Tested strains (NBRC - NITE Biological Resource Center, (NITE - National Institute of Technology and Evaluation) Tokyo, Japan; LMMiŚ - Laboratory of Molecular and Environmental Microbiology).

Species	Collection	Izolation year	Strain number
<i>N. fischeri</i> var. <i>fischeri</i>	NBRC 31895	1985	G90/14
<i>N. fischeri</i> var. <i>glabra</i>	NBRC 30572	1975	G91/14
<i>N. fischeri</i>	LMMiŚ	2014	G126/14
<i>N. fischeri</i>	LMMiŚ	2014	G128/14
<i>N. fischeri</i>	LMMiŚ	2014	G131/14
<i>N. fischeri</i>	LMMiŚ	2014	G153/14
<i>N. fischeri</i>	LMMiŚ	2014	G168/14

Studies revealed that all strains of *Neosartorya* grow after the heat shock. Five of the seven strains showed not significantly lower growth in reduced oxygen concentration. It was revealed intraspecific variation in metabolic profile of heat-resistant *Neosartorya fischeri* strains (Fig. 1). In general, tested strains utilized higher number of substrates in aerobic conditions compared to microaerophilic conditions (Fig. 2).

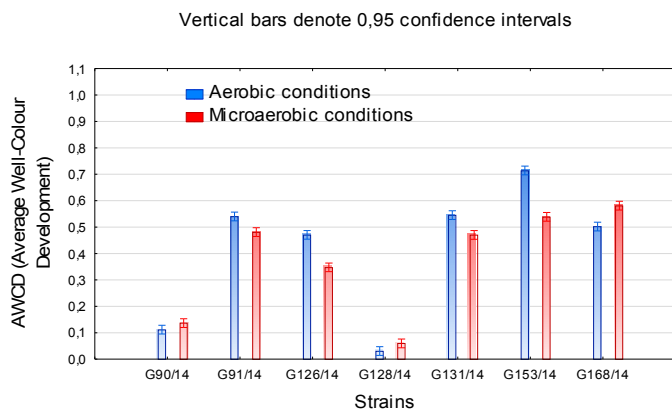


Fig.1 The metabolic profiles for particular isolates.

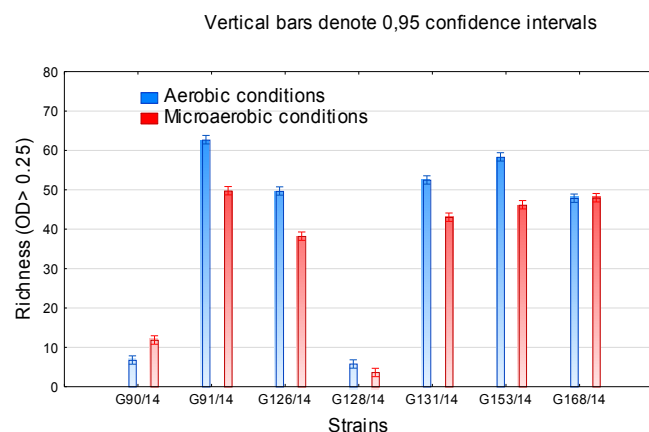


Fig.2. The number of substrate utilised by particular isolates.

Acknowledgement

The study was supported by National Science Centre (Poland), grant: DEC-2012/07/D/NZ9/03357

References

- [1] Dyer P.S., O’Gorman C.M., Sexual development and cryptic sexuality in fungi: insights from *Aspergillus* species. FEMS Microbiology Reviews, 2012, pp.165-192.
- [2] Fraç M., Jezierska-Tys S., Yaguchi T., Occurrence, detection, and characterization of heat-resistant fungi in soils and plants and their risk to human health. Advances in Agronomy, 2015, 132, pp.161-204.
- [3] Wyatt T. T., Gerwig G.J., Kamerling J.P., Wosten H.A.B., Dijksterhuis J., Structural analysis of novel trehalose-based oligosaccharides from extremely stress-tolerant ascospores of *Neosartorya fischeri* (*Aspergillus fischeri*). Carbohydrate Research, 2015, 411, pp.49-55.
- [4] Wyatt T.T., Leeuwen M.R., Golovina E.A., Hoekstra F.A., Kuenstner E.J., Palumbo E.A., Snyder N.L., Visagie C., Verkennis A., Hallsworth J.E., Wosten H.A.B., Dijksterhuis J., Functionality and prevalence of trehalose-based oligosaccharides as novel compatible solutes in ascospores of *Neosartorya fischeri* (*Aspergillus fischeri*) and other fungi. Environmental Microbiology, 2014, pp.1-17.
- [5] Panek. J., Fraç M., Bilińska-Wielgus N., Comparison of chemical sensitivity of fresh and long-stored heat resistant *Neosartorya fischeri* environmental isolates using BIOLOG Phenotype MicroArray System, PLOS ONE, 2015, 11, pp.1-19.

Influence of feedstock particle size on physical properties of solid biofuel from pine bark

Brunerová A., Brožek M.

Czech University of Life Sciences Prague, Kamýcká 129, 16521 Prague 6, Czech Republic

Corresponding author: Brunerová A., e-mail: brunerova@tf.czu.cz

Keywords: biomass, briquette, particle size, mechanical durability, rupture force

Abstract

Particle size is considered as an important feedstock property because it influences briquette moisture, content rupture force and mechanical durability, which is main indicator of physical quality of briquettes [1]. Despite this fact there is no defined range for optimal particle size. The diversity of suitable feedstocks indicate that it is necessary to perform a concrete measurements for specific feedstocks. Tree bark which is commonly used as a mulching bark, however there is a potential to use it as a feedstock for briquette production [2]. The aim of this paper was analyse the potential of waste bark as a feedstock for briquette production and stated the influence of different particle size on physical properties of bark briquettes.

Raw unprocessed material occurred in the form of large pieces with length 150mm in average and moisture content equal to 42.1%. This form did not allowed to use it for direct briquette production; material was dried in heated room to moisture content equal to approximately 10.0% in average. Subsequently was crushed by laboratory grinder to three types of particle sizes: <6mm (Group 1), 6-12mm (Group 2) and >12mm (Group 3) which was used for the production of three different kinds of briquette samples. All briquette samples were produced under the same manufacturing conditions into cylindrical shape with diameter equal to 50 mm by hydraulic piston press Briklis type BrikStar type 30–12 (Malšice city, Czech Republic) with following technical specifications: operating pressure 18 MPa, operating temperature 60°C and feedstock moisture content 8–15%. Specific measured and calculated properties of different particle size groups are noted in Tab. 1.

Tab. 1 Properties of briquette samples in average.

Particle size	Length (mm)	Weight (g)	Density ($\text{kg}\cdot\text{m}^{-3}$)
<6mm	56.98	115.44	953.25
6-12mm	55.89	111.79	929.69
>12mm	53.84	102.98	859.70

All procedures of feedstock preparation, processing, briquette production and subsequent testing and final evaluation of result values were performed in accordance to mandatory technical norms (namely International Standard EN ISO 17225–1:2015, EN 14918:2010, EN 18134-2:2016 and EN 15210–2:2011 [3–6]. During the experimental research a calorific value of briquette samples was estimated equal to $19.18\text{MJ}\cdot\text{kg}^{-1}$ in average which corresponds to mandatory minimal requirement ($17\text{MJ}\cdot\text{kg}^{-1}$) [4] at first and subsequently the briquette samples were subjected to tests for determination of their physical properties (moisture content, mechanical durability and rupture force). Final moisture content of briquette samples was tested by laboratory dryer LAC type S100/03 and results showed increasing of moisture content when feedstock particle size increases. Mechanical durability, defined as an ability of briquettes to remain intact during transportation, handling and storage [6], were experimentally tested in

dustproof rotating drum where they were subjected to controlled abrasion. Rupture force test which expresses force needed for briquette destruction was performed by universal tensile strength testing machine. Precise results values of described tests are noted in Tab. 2.

Tab. 2 Results of physical properties of different particle size groups in average.

Particle size	Mechanical durability (%)	Rupture force (N)	Moisture Content (%)
<6mm	91.9	2629.2	11.0
6-12mm	91.5	2663.5	12.4
>12mm	90.7	2287.2	12.3

Despite the fact that moisture content of final products should not exceed 10%, otherwise it can influence final briquette quality in negative way [5], [7], none of tested groups achieved required values. As is visible from Tab. 2 best result (lowest value) was measured for Group 1 with smallest particle size. All tested groups also showed great level of mechanical durability which corresponds to second highest level (>90.0%) and proves high level of briquette mechanical quality [6] admittedly best results exhibits Group 1. According to mechanical durability results this indicator increases with decreasing of particle size. Rupture force is not prescribed by any standard but as is visible from Tab. 2 best results were achieved by Group 2 with middle value of particle size. According to previous researches briquette quality increases with decreasing of feedstock particle size [1].

In conclusion, overall physical properties evaluation of pine bark briquettes exhibited satisfactory levels. In general in two cases from three exhibited best results Group 1 with smallest particle size and in one case of rupture force best results showed Group 2. It can be concluded that results differ in low level but still decreasing of particle size improves specific physical properties of briquettes.

References

- [1] H. Saptoadi, "The Best Biobriquette Dimension and its Particle Size," *Asian J. Energy Environ.*, vol. 9, no. 3, pp. 161–175, 2008.
- [2] W. Zribi, R. Aragüés, E. Medina, and J. M. Faci, "Efficiency of inorganic and organic mulching materials for soil evaporation control," *Soil Tillage Res.*, vol. 148, pp. 40–45, 2015.
- [3] ČSN EN ISO 17225-1, "Tuhá biopaliva - Specifikace a třídy paliv - Část 1: Obecné požadavky," *Praha: Český normalizační institut*, 2015.
- [4] ČSN EN 14918, "Tuhá biopaliva - Stanovení spalného tepla a výhřevnosti," *Praha: Český normalizační institut*, 2010.
- [5] ČSN EN 18134-2, "Tuhá biopaliva - Stanovení obsahu vody - Metoda sušení v sušárně - Část 2: Celková voda - Zjednodušená metoda," *Praha: Český normalizační institut*, 2016.
- [6] ČSN EN 15210-2, "Tuhá biopaliva - Stanovení mechanické odolnosti pelet a briket - Část 2: Brikety," *Praha: Český normalizační institut*, 2011.
- [7] J. S. Tumuluru, L. G. Tabil, Y. Song, K. L. Iroba, and V. Meda, "Impact of process conditions on the density and durability of wheat, oat, canola, and barley straw briquettes," *BioEnergy Res.*, vol. 8, no. 1, pp. 388–401, 2015.

Application of thermography and hyperspectral techniques for testing the resistance of tobacco (*Nicotiana Tabacum* L.) plants to the tobacco mosaic virus (TMV)

Gos M.¹, Siedliska A.¹, Zubik M.¹, Jędryczka M.², Baranowski P.¹

¹ Institute of Agrophysics, Polish Academy of Sciences, Doświadczalna 4, 20-290 Lublin, Poland

² Institute of Plant Genetics, Polish Academy of Sciences, Strzeszyńska 32, Poznań, Poland

Corresponding author: Gos M., e-mail: m.gos@ipan.lublin.pl

Keywords: thermography, hyperspectral imaging, tobacco, tobacco mosaic virus, NDVI

Abstract

Thermal imaging and hyperspectral imaging are two non invasive and non contact methods analysing physical - chemical properties of biological materials through the analysis of the visible and infrared radiations received from the studied materials (emitted or reflective) [1,2]. They are especially valuable for early detection of biotic stresses [3]. The main advantage of both methods is that they enable to analyse the spatial differentiation of radiation intensities within the studied objects giving the chance to detect local changes of tissues properties.

Tobacco mosaic virus (TMV) infects plants of Solanaceae family. The infection causes characteristic patterns on the leaves which are caused by local necrosis. The aim of the study was to evaluate the thermography and hyperspectral imaging as a non invasive methods for the detection of presymptomatic changes caused by tobacco mosaic virus (TMV) on three genotypes of *Nicotiana tabacum*, which differ with the levels of resistance to infection. Plants were grown in a growing chamber under controlled conditions (14 hour day-light photoperiod, 25/20°C day/night temperature, 70% air humidity). The material consisted of 30 plants at the same stage of development (8 weeks). In the experiment used two variants were created: 1) non inoculated plants, 2) plants inoculated with TMV. The experiments were performed for 21 days to follow full stage of plant reaction to pathogen. The thermography analysis were performed using the camera SC620, MWIR range (8-13µm), (FLIR Systems, Inc., USA); hyperspectral imaging was done using VNIR camera (400-1000 nm) with spectrometer ImSpector V10E and SWIR camera (1000-2500nm) with spectrometer N25E 2/3", (SPECIM, Finland).

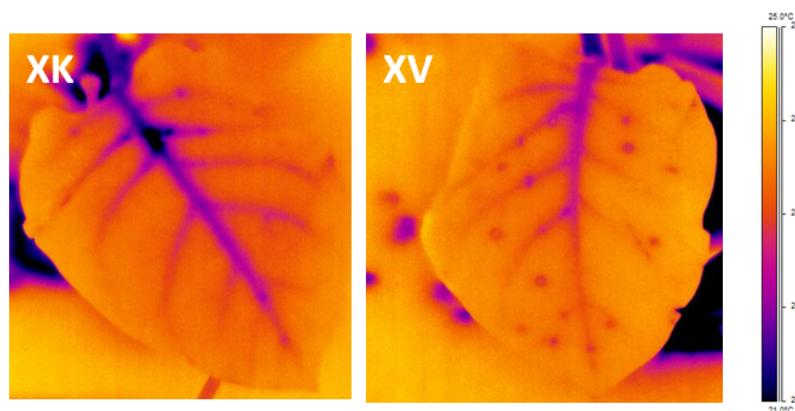


Fig. 1 Thermal images of leaves of Xanthi (X) genotype: control (XK), a plant infected with a virus (XV)

Fig. 1 shows the thermal image of non infected (XK) and infected (XV) leaves of plants (Xanthi species). As can be seen, the thermal distribution clearly indicate leaf areas with lower temperature values, correlated with necrosis. The low temperature areas may correspond to limiting rate of leaf transpiration. The

necrotic changes do not occur in a genotype Petit Havana (SH), but infected plants have a higher

temperature than non inoculated one. Results obtained from the experiment confirm the usefulness of thermographic technique for non invasive detection of the leaf reaction to pathogen.

The second method used to monitor plant reaction to pathogen was a hyperspectral imaging techniques. All hyperspectral image pixels are represented by a reflectance spectra. The spectra allows to obtain the information about the vegetative state of plants. It is possible to calculate the normalized difference vegetation index (NDVI) (equation 1), which is a normalized ratio of the NIR (near infrared) and red bands [4].

$$NDVI = \frac{(R_{800} - R_{680})}{(R_{800} + R_{680})} \quad (1)$$

The NDVI value changes during infection development reflects plant reaction kinetic and

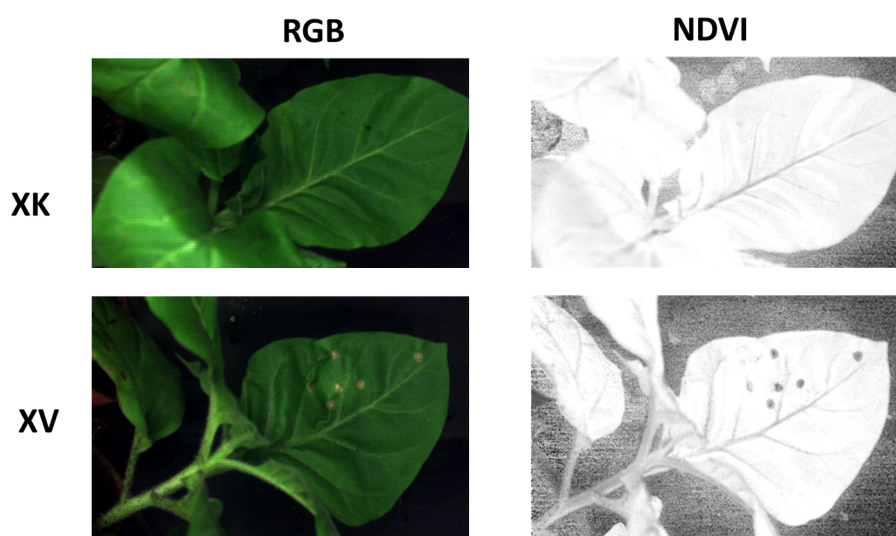


Fig. 2 Hyperspectral images of the normalized difference vegetation index (NDVI) of Xanthi (X) genotype: control (XK), a plant infected with the TMV

resistance to pathogen (Fig. 2).

Thermal imaging differentiate cultivars of tobacco infected with TMV. The results obtained by hyperspectral imaging indicate that Petit Havana tobacco species has a slower reaction to infection.

References

- [1] Walczak T., Baranowski,P., Mazurek.W., Application of thermography in Agrophysics, Training Course for Young Research Workers' Physicochemical and Physical Methods of Studies of Soil and Plant Materials. Theory and Practice ", IAPAS, Lublin, 2003., pp. 111-117.
- [2] Baranowski,P., Mazurek,W., Jędrzycka,M., Babula-Skowrońska,D., Temperature changes of oilseed rape (*Brassica napus*) leaves infected by fungi of *Alternaria* sp., *Oilseed Crops*, 2009, 30 (1), pp. 21-33.
- [3] Baranowski,P., Lipecki,J., Mazurek,W., Walczak,R.T., Detection of mechanical damage to apples with the use of thermography, *Acta Agrophysica*, 2005, 6 (1), pp. 19-29.
- [4] Rouse J.W., Haas R.H., Schell J.A., Deering D.W., Monitoring vegetation systems in the Great Plains with ERTS. In: Fraden S.C., Marcanti E.P. & Becker M.A. (eds.), Third ERTS-1 Symposium, 10–14 Dec. 1973, NASA SP-351, Washington D.C. NASA, 1974, pp. 309–317.

Effect of various factors on selected fermented wort rheologic properties

Hlaváč P., Božiková M.

Slovak University of Agriculture in Nitra, Tr. A. Hlinku 2, 949 76 Nitra, Slovakia

Corresponding author: Hlaváč P., e-mail: Peter.Hlavac@is.uniag.sk

Keywords: fermented wort, influencing factors, dynamic viscosity, activation energy

Abstract

Wort is the liquid extracted from the mashing process during the brewing of beer or whisky. Sugars contained in wort are changed to alcohol by the brewing yeasts during fermentation. Chemical properties of wort are published by many authors, but its physical properties are almost impossible to find. Mentioned are only some physical properties of beer. High viscosity and other factors can affect fermentability of wort [2]. Authors also found that the dynamic viscosity values of malt wort samples were in range (1.42 – 2.01) mPa·s at 15 °C. The influence of germination time and temperature on the properties of rye malt and rye malt based worts were examined by authors [5]. They found out that dynamic viscosity of rye malt based worts had higher values than barley malt based worts. The amounts of sugar levels and alcohols during wort fermentation were monitored by researchers [7]. They proved that amount of sugars is decreasing during fermentation, while the amount of alcohol is increasing. The advantages of maltose fermentation at low temperatures using special type of yeasts were described by authors [4]. They had also determined activation energy of maltose fermentation by yeasts cell free and immobilized. Influence of aging or storing of beer was examined by many authors [1], [8], [9], etc.

This research was oriented on rheological properties which are very complicated characteristics of materials. Examined were selected rheologic properties such as dynamic viscosity and activation energy. Viscosity as one of the most important rheologic parameters is defined as the resistance of a fluid to flow. The unit of dynamic viscosity in SI units is Pa·s. The temperature effect on viscosity can be described by an Arrhenius type equation

$$\eta = \eta_0 e^{-\frac{E_A}{RT}} \quad (1)$$

where η_0 is reference value of dynamic viscosity, E_A is activation energy, R is gas constant and T is absolute temperature [3]. Activation energy is more readily audible at higher temperatures and the fluid flows easily. In chemistry, activation energy means the amount of energy that is required to activate atoms or molecules to a condition in which they can undergo chemical transformation or physical transport. In terms of the transition-state theory, activation energy is the difference in energy content between atoms or molecules in an activated or transition-state configuration and the corresponding atoms and molecules in their initial configuration. Activation energies are determined experimentally at different temperatures [6].

Influence of various factors as temperature, fermentation time and storing time on analysed rheologic properties was searched. In our research we analyzed two wort samples. First sample was taken at the beginning of fermentation and second sample after three hours of fermentation. Both samples were also measured after three weeks of storing. Measured samples were cooled to temperature 5 °C and dynamic viscosity was measured in temperature range (7 – 30) °C. Measuring of dynamic viscosity was performed by digital viscometer Anton Paar (DV-3P). Temperature dependencies of dynamic viscosity can be described by decreasing exponential functions (2) in measured temperature range.

$$\eta = A e^{-B\left(\frac{t}{t_0}\right)} \quad (2)$$

In case that $\eta_0 = A$, Eq. 1 and Eq. 2 can be used for calculation of activation energy at different temperatures. Temperature dependencies of activation energy can be described by a linear increasing function (3) in analysed temperature range.

$$E_A = C\left(\frac{t}{t_0}\right) - D \quad (3)$$

where t is temperature, t_0 is 1 °C, A , B , C , D are constants dependent on kind of material, and on ways of processing and storing.

Our results of wort dynamic viscosity are in good agreement with authors [2]. We found out that dynamic viscosity of second sample of wort (after three hours of fermentation) is lower than for first sample (without fermentation) and also that difference was bigger after storing. Activation energy had decreased a bit after fermentation, but it was more visible after storing. So the fermentation process and storing had caused the decrease of both analysed parameters: dynamic viscosity and activation energy. This was caused by structural changes in wort during fermentation and storing.

Acknowledgement

This work was supported by Research Centre AgroBioTech built in accordance with the project Building Research Centre „AgroBioTech” ITMS 26220220180.

References

- [1] Caballero I., Blanco C. A., Porras M., Iso- α -acids, bitterness and loss of beer quality during storage. *Trends in Food Science and Technology*, 2012, 26, pp. 21 – 30.
- [2] Edney M. J., Eglinton J. K., Collins H. M., Barr A. R., Legge W. G., Rossnagel B. G., Importance of endosperm modification for malt wort fermentability. *Journal of the Institute of Brewing*, 2007, 113(2), pp. 228 – 238.
- [3] Figura L. O., Teixeira A. A., *Food Physics, Physical properties – measurement and applications*, Springer, USA, 2007, 550 pages, ISBN 978-3-540-34191-8.
- [4] Ganatsios V., Koutinas A. A., Bekatorou A., Kanellaki M., Nigam P., Promotion of maltose fermentation at extremely low temperatures using a cryotolerant *Saccharomyces cerevisiae* strain immobilized on porous cellulosic material. *Enzyme and Microbial Technology*, 2014, 66, pp. 56 – 59.
- [5] Hübner F., Schehl B. D., Gebruers K., Courtin Ch. M., Delcour J. A., Arendt E. K., Influence of germination time and temperature on the properties of rye malt and rye malt based worts. *Journal of Cereal Science*, 2010, 52, pp. 72 – 79.
- [6] Mansur G. A. et al., *Encyclopaedia Britannica*, 2014, available at <http://www.britannica.com/EBchecked/topic/4535/activation-energy>
- [7] Monošík R., Magdolen P., Stred'anský M., Šturdík E., Monitoring of monosaccharides, oligosaccharides, ethanol and glycerol during wort fermentation by biosensors, HPLC and spectrophotometry. *Food chemistry*, 2013, 138, pp. 220 – 226.
- [8] Nimubona D., Blanco C. A., Caballero I., Rojas A., Andrés-Iglesias C., An approximate shelf life prediction of elaborated lager beer in terms of degradation of its iso- α -acids. *Journal of Food Engineering*, 2013, 116, pp. 138 – 143.
- [9] Vanderhaegen B., Neven H., Verachtert H., Derdelinckx G., The chemistry of beer aging – a critical review. *Food Chemistry*, 2006, 95, pp. 357 – 381.

Visco-elastic and elastic-plastic contact interactions of seeds during impacts

Horabik J.

Institute of Agrophysics Polish Academy of Sciences, Doświadczalna 4, 20-290 Lublin, Poland

Corresponding author: Horabik J., j.horabik@ipan.lublin.pl

Keywords: contact models, seeds, impact

Abstract

Agriculture and food processing are among the biggest producers of raw materials and final products in the form of granular materials. The majority of products pass a processing chain from the harvest to the consumer in the form of granular solids. Chain of technological operations like, harvest, transport, storage, segregation, screening involve grain-grain or grain-construction impacts. To describe and predict precisely behavior of particles profound understanding of mechanics of impact interactions of particles is necessary.

During impacts accumulation and dissipation of mechanical energy occurs: accumulation of potential energy of elastic deformation and energy dissipation in viscous and plastic deformation, and in frictional displacements and rotations. The behavior of agricultural materials differs from the behavior of other materials mainly because of their biological origin. Granular materials of biological are distinguished by large deformability of particles and strong dependence of their mechanical properties on moisture content. Contrary to materials of mineral origin, moisture penetrates inside the grain, leading, in some cases, to qualitative changes in physical properties. With the moisture content increase behavior of seeds changes from elastic-plastic, through ductile, to visco-elastic. Impact force versus impact time is usually unsymmetrical. The ratio of the fall time of the impact force pulse to the rise time, TR , provides a convenient criterion for the selection between elastic-plastic models appropriate for dry seed ($F/R < 1$) and visco-elastic models describing behavior of wet seed ($F/R > 1$) [6]. In the case of dry seeds the F/R ratio was decreasing with impact velocity increase which is in a good agreement with predictions of elastic-plastic model of Thornton and Ning [4] involving elastic contact of Hertz and plastic yielding on the central part of contact area and elastic unloading. In the case of wet seeds the F/R ratio was independent on impact velocity (Fig. 1). This property of wet seeds is predicted by visco-elastic contact model of Tsuji et al. [5] in which displacement in the dissipative component of the model is in power of 0.25.

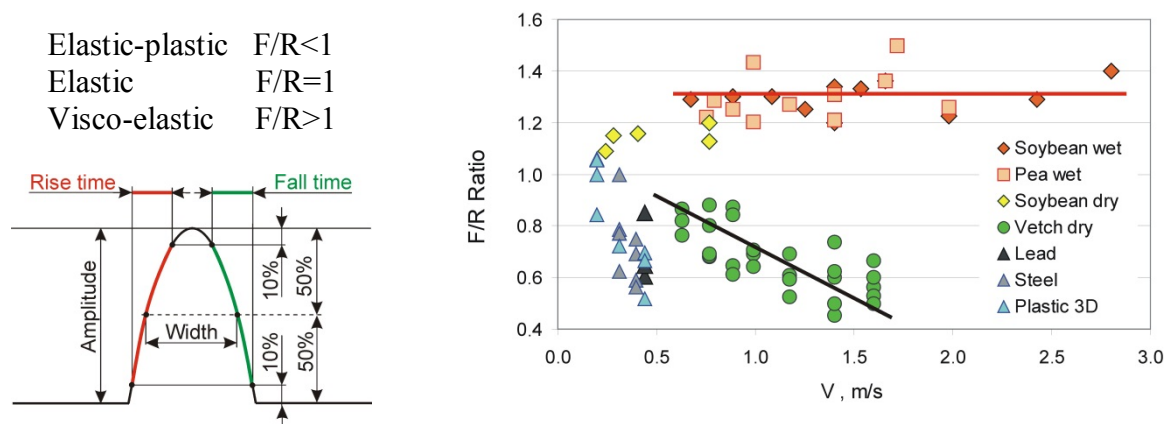


Fig. 1. The F/R ratio as the parameter of distinguishing two mechanisms of impact behavior of seeds: elastic-plastic and visco-elastic.

Visco-elastic models with different exponent of power of displacement in dissipative component of 0.25 [5], 0.5 [3], 1 [1] to 1.5 [2] revealed different degree of agreement with

experimental data in asymmetry of impact force impulse and dependence of the restitution coefficient on impact velocity. Exponent of 0.25 provides restitution coefficient and F/R Ratio independent on impact velocity. Experimental data indicates that the F/R Ratio of impacts of wet seeds is independent on impact velocity while the restitution coefficient decreases with impact velocity increase (Fig. 2). The best fitting was provided by the visco-elastic model with the exponent of 1.5. That two characteristics of seeds impact behavior, independence of the F/R Ratio and mutual strong dependence of the restitution coefficient on impact velocity, cannot be predicted simultaneously by the same visco-elastic model.

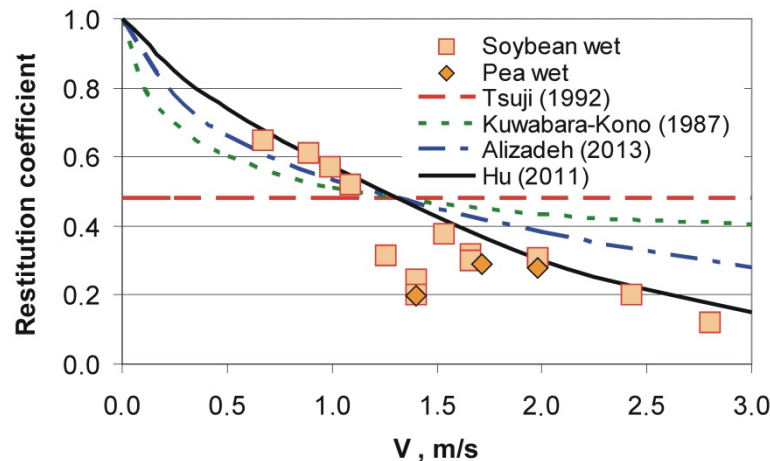


Fig. 2. Restitution coefficient of soybean and pea seeds compared to predicted by several models as influenced by impact velocity.

Conclusions:

1. The F/R ratio allows to distinguish two mechanisms of impact behavior of seeds: elastic-plastic ($F/R < 1$) and visco-elastic ($F/R > 1$).
2. In the case wet seeds asymmetry of impact force-time relationship was found to be independent on impact velocity while the restitution coefficient was decreasing with impact velocity increase.

References

- [1] Alizadeh E., Bertrand F., Chaouki J., Development of a granular normal contact force model based on a non-Newtonian liquid filled dashpot. *Powder Technol.*, 2013, 237, pp. 202–212.
- [2] Hu G., Hu Z., Jian B., Liu L., Wan H., On the Determination of the Damping Coefficient of Non-linear Spring-dashpot System to Model Hertz Contact for Simulation by Discrete Element Method. *J. Computers*, 2011, 6 (5), pp. 984–988.
- [3] Kuwabara G., Kono K., Restitution coefficient in a collision between 2 spheres. *Japanese Journal of Applied Physics*, 1987, **26**, pp.1230–1233.
- [4] Thornton C., Ning Z., A theoretical model for the stick/bounce behaviour of adhesive, elastic-plastic spheres. *Powder Technol.*, 1998, 99(2), pp. 154–162.
- [5] Tsuji Y., Tanaka T., Ishida T., Lagrangian numerical simulation of plug flow of cohesionless particles in a horizontal pipe. *Powder Technol.*, 1992, 71, pp. 239–250.
- [6] Wojtkowski M., Pecun J., Horabik J., Molenda M., Rapeseed impact against a flat surface: Physical testing and DEM simulation with two contact models. *Powder Technol.*, 2010, 198, pp. 61–68.

Periphyton Communities In Wastewater Treatment In Lublin (Poland) – Case Study

Jaromin-Gleń K.¹, Babko R.², Kuzmina T.³, Łagód G.⁴, Bieganowski A.¹

¹ Institute of Agrophysics, Polish Academy of Sciences, Doświadczalna 4, 20-290 Lublin, Poland

² Schmalhausen Institute of Zoology NAS of Ukraine, B. Khmelnytsky Str. 15, Kiev, 01601, Ukraine

³ Sumy State University, Rymskogo-Korsakova Str. 2, Sumy, 40007, Ukraine

⁴ Lublin University of Technology, Nadbystrzycka 40B, 20-618 Lublin, Poland

Corresponding author: Jaromin-Gleń K., e-mail: k.jaromin-glen@ipan.lublin.pl

Keywords: wastewater treatment plant, periphyton, activated sludge

Abstract

The function of activated sludge is supported by organisms developing in all wastewater treatment devices of the wastewater treatment plant (WWTP). These organisms are defined as periphyton, which inhabits available ecological niches even against actions undertaken by technologists. Periphyton is a supplementary element of the ecosystem in the individual stages of the process in a WWTP. It may be suspected that the structure of periphyton (the abundance and/or composition) depends on environmental factors, which, in turn, are dependent on e.g. the result of the treatment process [1,3]. Furthermore, the investigations of the structure of biological populations are also reported by means of relevant indices [2,4]. The main goal of this study was to identify the structure

of periphyton in the successive stages of the WWTP in Lublin (Poland) during the treatment process run with the activated sludge method. The research material was taken from 11 points - successive devices of the municipal “Hajdów” WWTP in Lublin (Poland). The sampling sites are shown in Figure 1.

These were:

1. pre-screen chamber,
2. post-screen chamber,
3. pre-grit separator chamber,
4. post-grit separator chamber,
5. primary clarifier,
6. anaerobic bioreactor chamber,
7. anoxic chamber,
8. aerobic bioreactor chamber,
9. bioreactor outlet,
10. secondary clarifier,
11. channel discharging to the receiver.

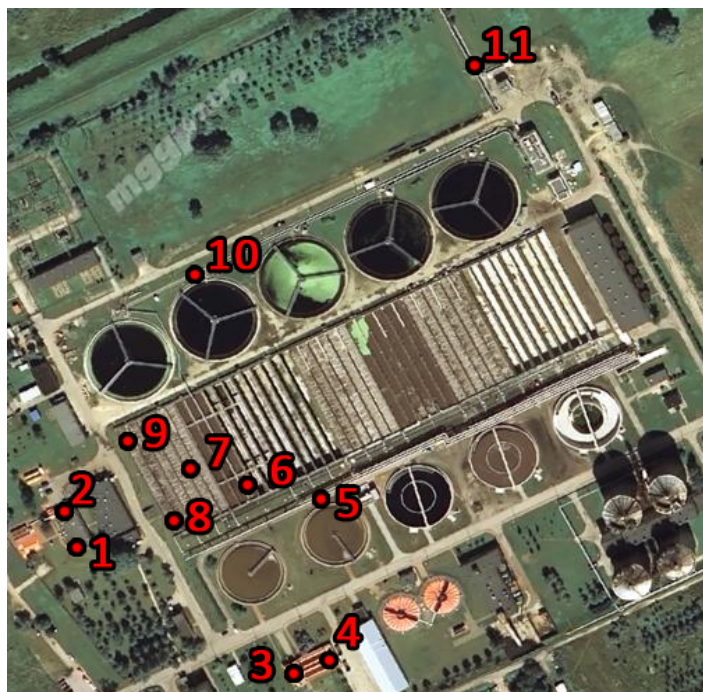


Fig. 1 Schema of WWTP with marked sampling points

The samples were taken ca. 15 cm below the sewage surface in each place. Each bottle was filled with a suspension of sewage (1/3 of the total volume) from the point of sampling. The samples were analysed under a transmitted-light bright-field optical microscope with a magnification of 100, 250, and 400x.

Information about the abundance of periphyton organisms in the successive devices of the WWTP in Lublin is shown in Figure 2.

Figure 2 shows the number of specimens of the periphyton organisms in the selected devices of the “Hajdów” WWTP. It should be noted that there are three most numerous points: the secondary clarifier, primary clarifier, and the channel discharging wastewater to the receiver (5, 10 and 11), in which the number of organisms is 39 000, 75 000, and 38 000 ind/cm³, respectively. The changes can be related to the different availability of light and oxygen in those devices.

The following conclusion:

1. The structure of the periphyton changes in the subsequent devices of the technological wastewater treatment system.
2. The changes are determined by the contact with the community of activated sludge organisms in the biological stage of treatment.

References

- [1] Jaromin, K., Babko, R., Łagód, G., Abundances of protozoa on particular devices of “Hajdów” WWTP on the background of the nitrogen compounds concentration. *Proceedings of ECOpole*, 2010, 4(2), pp. 403-408.
- [2] Łagód, G., Chomczyńska, M., Montusiewicz, A., Malicki, J., Bieganowski, A., The proposal of measurement and visualization methods for dominance structures in the saprobe communities. *Ecological Chemistry and Engineering*, S, 2009, 16(3):, pp. 369-371.
- [3] Łagód, G., Jaromin, K., Kopertowska, A., Plizga, O., Lefanowicz, A., Woś, P. Bioindicative studies of pecton in selected facilities of the Hajdów Wastewater Treatment Plant – a case study. In L. Pawłowski, M. Dudzińska and A. Pawłowki, Eds., *Environment Engineering III*. London: CRC Press/Balkema, Taylor & Francis Group, 2010, p. 618.
- [4] Madoni, P. A sludge biotic index (SBI) for the evaluation of the biological performance of activated-sludge plants based on the microfauna analysis. *Water Research.*, 1994, 28(1):, pp. 67-75.

Number of specimen (ind/cm³)

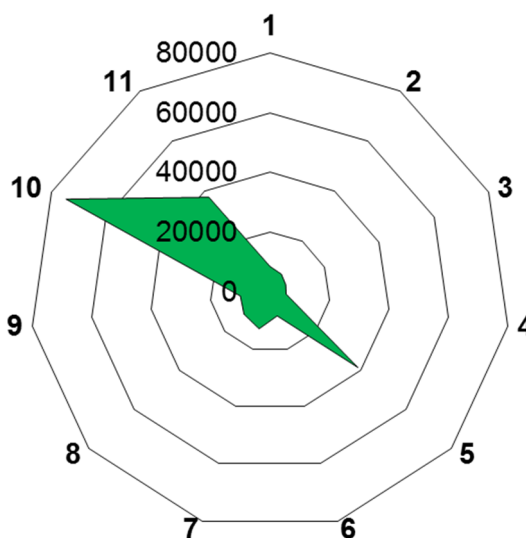


Fig. 2 Total number of specimen of periphyton organisms WWTP in Lublin

Mechanical Behaviour and Loading Curves of Selected Bulk Oilseeds under Linear Compression

Kabutey, A.¹, Herák, D.¹, Sigalingging, R.², Divišová, M.¹

¹ Faculty of Engineering, Department of Mechanical Engineering, Czech University of Life Sciences Prague, Kamycka 129, Praha 6, Czech Republic

Tel: +420 775 661 481; Email: kabutey@tf.czu.cz

² Faculty of Agriculture, Department of Agricultural Engineering, University of Sumatera Utara, Medan, Indonesia

Corresponding author: Kabutey A., e-mail: kabutey@tf.czu.cz

Keywords: Oilseeds pressing, oil yield, energy efficiency, mathematical model

Abstract

Comprehensive information on mechanical properties and load-deformation curves of oilseed crops under compression loading will improve the cost-effectiveness of oil extraction technology. In this communication highlight briefly our published studies in scientific journals indexed in Scopus and Web of science. The research mainly focused on bulk oilseeds of jatropha, rape, sunflower and palm kernels.

Biofuel production of vegetable oilseeds is among the sustainable energy sources of energy efficiency for the present and next generations. Designing an efficient oil extraction technologies has been a rising concern to both researchers and engineers. Understanding the mechanical behaviour and deformation characteristic curves of bulk oilseeds or kernels under compression loading and also the development of suitable mathematical models for their description is a step toward the oil processing technology optimization. Considerable studies in the literature [1-5] have been carried out on the subject, however, more studies need to be conducted in the future.

Bulk oilseeds of jatropha, rape and sunflower as well as palm kernels have been evaluated under compression test using a universal compressive device in terms of maximum deformation and deformation curves, energy and energy density as well as oil yield at varying speeds (1 to 60 mm min⁻¹), seeds moisture content (1 to 37% w.b), compressive forces (30 to 250 kN), bulk seeds pressing heights (20 to 80 mm) and pressing vessel diameters (40 to 100 mm).

Seed moisture content higher than 10% w.b. causes serration effect on the load-deformation curves [1]. Smaller vessel diameters 40 and 60 mm also exhibit serration effect unlike bigger diameters 80 and 100 mm which give smooth curve behaviour [1,3]. The serration effect thus influences oil yield and also contributes to the cessation of the compression process [1]. Under the load-deformation curve, two pressing areas can be described in relation to moisture content and vessel diameters which are the increasing region with maximum oil where energy utilization is efficient and the region with serration without oil leading to inefficient energy utilization [3]. Lower and upper oil points can be identified on the load-deformation curve where the oil point energy increases with increasing speed [1,5]. Seed deformation, energy and energy density together with oil yield increases directly with vessel diameter and bulk seeds pressing height. Maximum compressive force is required to deform roasted palm kernels for higher percentage kernel oil. Higher oil yield is achieved at lower speed [1]. Tangent curve mathematical model can be used for fitting the load-deformation curves as well as the amount of energy which is the area under the curve [2,4,5]. The findings from the linear compression should be transferred to the non-linear environment involving mechanical screw presses for accurate evaluation. The results will therefore help engineers to design efficient oil expression system. However, strong research collaboration should be promoted and strengthened between

researchers, engineers and oil processing industries.

References

- [1] Kabutey, A., Herák, D., Chotěborský, R., Sigalingging, R., Mizera, Č., Effect of compression speed on energy requirement and oil yield of *Jatropha curcas* L. bulk seeds under linear compression. *Biosystems Engineering*, 2015, 136, pp. 8-13.
- [2] Sigalingging, R., Herák, D., Kabutey, A., Dajbych, O., Hrabě P., Mizera, Č., Application of a tangent curve mathematical model for analysis of the mechanical behaviour of sunflower bulk seeds. *International Agrophysics*, 2015, 29(4), pp.517-524.
- [3] Divišová, M., Herák, D., Kabutey, A., Sigalingging, R., Svatoňová, T., Deformation curve characteristics of rapeseeds and sunflower seeds under compression loading. *Scientia Agriculturae Bohemica*, 2014, 45(3), pp.180-186.
- [4] Herák, D., Kabutey, A., Divišová, M., Simanjuntak, S., Mathematical model of mechanical behaviour of *Jatropha curcas* L. seeds under compression loading. *Biosystems Engineering*, 2013, 114(3), pp.279-288.
- [5] Herak, D., Kabutey, A., Hrabe, P., Oil point determination of *Jatropha curcas* L. bulk seeds under compression loading. *Biosystems Engineering*, 2013, 116(4), pp.470-477.

The size and electrophoretic mobility of the biosurfactant aggregates at a different salt concentration

Koczańska M., Cieśla J., Bieganowski A.

Institute of Agrophysics, Polish Academy of Sciences, Doświadczalna 4, 20-290 Lublin, Poland

Corresponding authors: Koczańska M., e-mail: m.koczanska@ipan.lublin.pl,

Cieśla J., e-mail: j.ciesla@ipan.lublin.pl

Keywords: electrophoretic mobility, ionic strength, particles size, rhamnolipid

Abstract

Biosurfactants, a group of surface active agents produced by microorganisms, have similar properties to classical surfactants (e.g. they are able to lower the surface tension and enhance the solubility of slightly soluble substances). However, they are more biodegradable and aggregate at much more lower concentration (CMC - Critical Micelle Concentration) than classical surfactants. The CMC of rhamnolipid is about 10 times lower than this of sodium dodecyl sulfate (SDS, an anionic surfactant) at pH=6.2 [1]. Such properties predestine the biosurfactants to replace the chemical surface active agents, which have been used so far, e.g. in the composition of pesticides and substances used for soil remediation [2,3].

Rhamnolipids are a type of glycolipid biosurfactants which can be produced by various bacterial species. These substances which are synthesized by *Pseudomonas aeruginosa* are a mixture of mono- and di-rhamnolipids. The chemical structure of the rhamnolipids molecules is shown in Fig. 1.

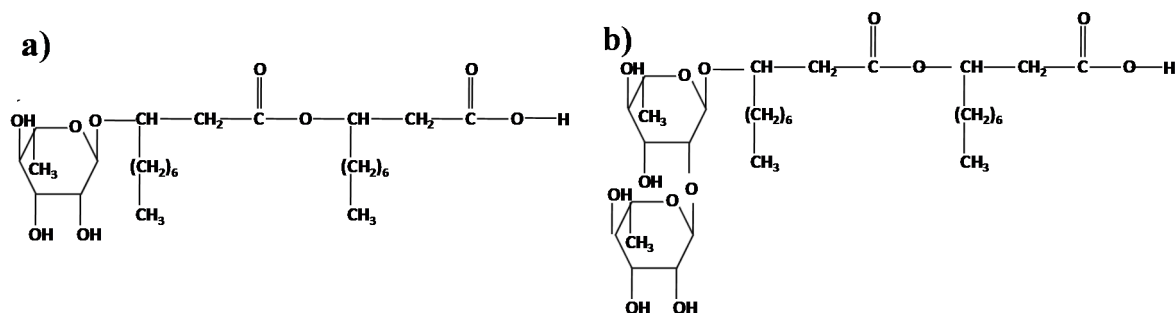


Fig. 1. The chemical structure of mono- (a) and di-rhamnolipids (b).

Due to the presence of acidic functional groups in this biosurfactant molecule the aggregation process and stability of the rhamnolipid micelles depends on the pH and ionic strength of solution. An information about the surface charge of aggregates can be obtained by the determination such electrokinetic properties as electrophoretic mobility. It describes the movement of particles dispersed in liquid under the influence of applied electric field. The concentration of surrounding medium (ionic strength) modifies the thickness of ionic atmosphere in the particle/medium interface and, in a consequence, the value of electrophoretic mobility [4]. However, the rhamnolipids are not detailedly characterized according to that.

Present work is focused on description of the impact of salt concentration on the size and electrophoretic mobility of the rhamnolipid aggregates in solutions at different pH.

Commercially available Rhamnolipid R-95 (AGAE Technologies, USA; Sigma Aldrich Poland) was used for preparation of micellar solutions (the concentrations of biosurfactant were higher than CMC at the given pH conditions). The ionic strength (10^{-3} M – 10^{-1} M) and pH (5.5 – 6.5) were adjusted by the addition of KCl and H_2SO_4

or KOH, respectively.

Particles size (Dynamic Light Scattering method) and electrophoretic mobility (Laser Doppler Velocimetry method) of rhamnolipids solutions were determined using a Zetasizer Nano ZS (Malvern Ltd., UK) at 20°C. Three independent measurements were performed each time and the mean results was calculated.

The examples of the results which illustrate the change of size of aggregates (mean hydrodynamic diameter) and electrophoretic mobility with the increasing ionic strength of medium are shown in Fig. 2.

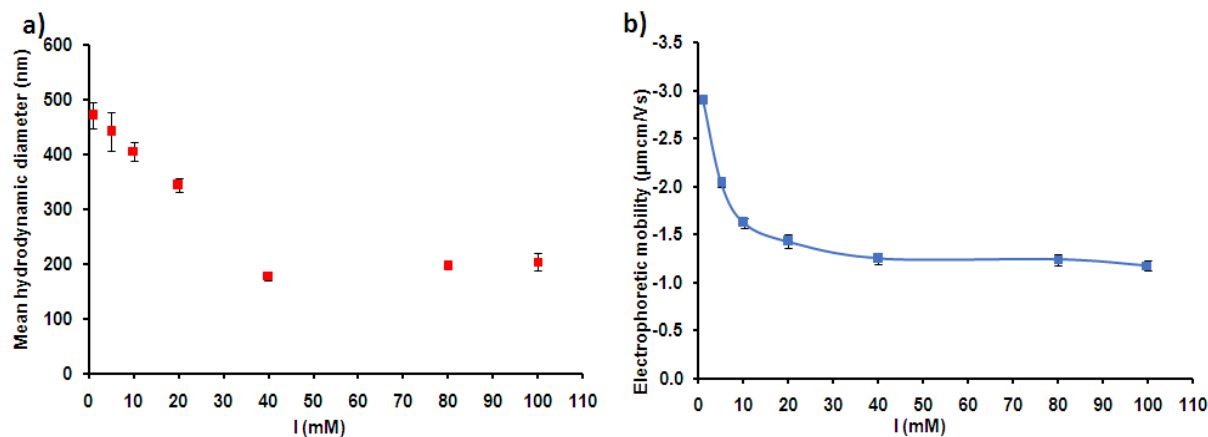


Fig. 2. Dependence of a) the mean hydrodynamic diameter and b) electrophoretic mobility on the ionic strength of dispersing medium for the micellar solution of rhamnolipid (160 mg/l) at pH = 5.5.

A negative values of electrophoretic mobility revealed that rhamnolipid is an anionic biosurfactant and form negatively charged aggregates. Moreover, electrokinetic properties and the size of rhamnolipid micelles at a particular pH of solution were dependent on the ionic strength. It was mainly due to the increase of the compactness of the electrical double layer with the increasing salt concentration.

References

- [1] Özdemir G., Sezgin Ö.E., Keratin–rhamnolipids and keratin–sodium dodecyl sulfate interactions at the air/water interface. *Colloids and Surfaces B: Biointerfaces*, 2006, 52, pp. 1-7.
- [2] Akintunde T.A., Abioye O.P., Oyeleke S.B., Boboye B.E., Ijah U.J.J., Remediation of Iron Using Rhamnolipid-Surfactant Produced by *Pseudomonas aeruginosa*. *Research Journal of Environmental Sciences*, 2015, 9, pp. 169-177.
- [3] Sachdev D.P., Cameotra S.S., Biosurfactants in agriculture. *Applied Microbiology and Biotechnology*, 2013, 97, pp. 1005–1016.
- [4] Ohshima H., Electrophoretic mobility of soft particles. *Colloids Surfaces A: Physicochemical and Engineering Aspects*, 1995, 103, pp. 249-255.

Behavior of photovoltaic system during solar eclipse

Kouřim P., Libra M., Poulek V.

Czech University of Life Sciences Prague, Kamýcká 129, 16521 Prague 6, Czech Republic

Corresponding author: Kouřim P., e-mail: kourim@tf.czu.cz

Keywords: solar eclipse, photovoltaics, PV system

Abstract

PV power plants have been recently installed in very large scale. So the effects of the solar eclipse are of big importance especially for grid connected photovoltaic (PV) systems. There was a partial solar eclipse in Prague on 20th March 2015. We have evaluated the data from our facility in order to monitor the impact of this natural phenomenon on the behavior of PV system (see Figs. 1, 2 and Tab. 1, 2). The behavior of PV system corresponds with the theoretical assumption. The power decrease of the PV array corresponds with the relative size of the solar eclipse. $I-V$ characteristics of the PV panel correspond to the theoretical model presented in our previous work [1]. Analysis of the behaviour of PV systems under partial shading was published in papers [2-3].

Also, thanks to the favorable weather on 19th to 20th March 2015, we were able to observe the behavior of PV system during the solar eclipse. Monitoring of the data during two consecutive sunny days, including the solar eclipse, shows excellent agreement of theory and experiment.

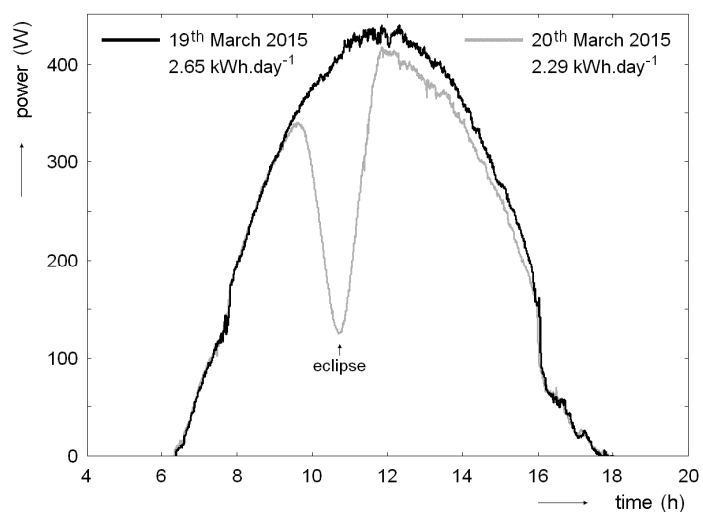


Fig. 1 Timeseries of instantaneous output power and the amount of generated electric energy

- Decrease of the instantaneous output power of the PV system during the solar eclipse corresponds with the relative shading of the solar disc and with decrease of the intensity of solar radiation.
- A lower value of instantaneous output power after the eclipse may be associated with the condensation of water vapor in atmosphere due to the decrease of air temperature during eclipse and with the higher absorption in the near infrared region of the spectrum.
- Temperature of PV panels corresponds mainly with the radiation intensity, but it is also influenced by the wind speed and therefore by natural cooling.
- behavior of $I-V$ characteristics of PV panel corresponds with the theoretical model based on the theory of semiconductors.
- Solar eclipse has a significant impact on the energy sector of some countries focused on renewable energy sources. The drop in performance PV power plants have to be balanced and covered from other sources.

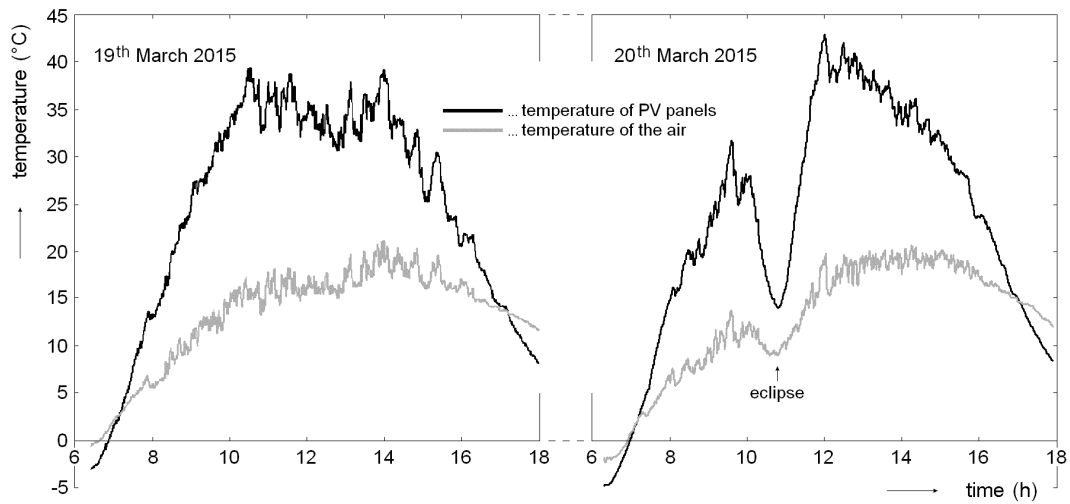


Fig. 2 Timeseries of PV panels temperature and air temperature

Tab. 1 Selected values of important variables during the solar eclipse on March 20, 2015

Eclipse phase	Time (h)	Solar disk coverage (%)	Sun height (°)	Sun azimuth (°)	Angle of incidence of sun rays on PV panels (°)
start	9:37	0	30	134	39
maximum	10:46	68	37	154	21
finish	11:58	0	40	176	5

Tab. 2 Selected values of important variables during the solar eclipse on March 20, 2015

Eclipse phase	Time (h)	Solar radiation intensity - horizontal plane (W.m ⁻²)	Solar radiation intensity on perpendicular plane (W.m ⁻²)	Solar radiation intensity on PV panels (W.m ⁻²)	Temperature of PV panels (°C)	Instantaneous output power (W)
start	9:37	437	874	679	31	340
maximum	10:46	155	258	241	14	124
finish	11:58	612	952	948	43	415

Acknowledgement

The work was supported by the internal research project of the Faculty of Engineering IGA 2015: 31120/1312/3103.

References

- [1] Poulek, V., Libra, M., Photovoltaics. ILSA, Prague, Czech Republic, 2010, 169 p. ISBN 978-80-904311-2-6.
- [2] Wang, Y. J., Sheu, R. L., Probabilistic Modeling of Partial Shading of Photovoltaic Arrays. International Journal of Photoenergy, 2015, Article ID 863637, pp.1-10.
- [3] He, W. et al., Safety Analysis of Solar Module under Partial Shading. International Journal of Photoenergy, 2015, Article ID 907282, pp.1-8.

Compressive Properties of Pellets

Kubík L.

Department of Physic, Slovak University of Agriculture in Nitra, Tr. A. Hlinku 2, 949 76 Nitra, Slovak Republic, tel.:+421376414879

Corresponding author: Kubík, L., e-mail: Lubomir.Kubik@uniag.sk

Keywords: compressive properties; pellets; stress, strain

Abstract

Pellet strength as well as fracture surface analysis provide insight into the level and type of internal bonding. Breaking the pellets using the low speed in the compression test and the higher speed of breaking the pellet manually may have different mechanisms of failure since the polymers show viscoelastic behavior [3]. By pelletization, raw biomass can be converted into a pellet form with improved fuel quality such as increased bulk density, and uniformed shape and size [2]. Pellets which were made using the straw and hays were prepared by mixing plant residues with spruce shavings as well as from pure materials, i.e. wheat straw, hay and sawdust [1]. Cylinder pellet samples were made from hay by the granulating machine MGL 200 (Kovonovak). The pellets were submitted to compressive loading. The compressive loading curves of dependencies of force on strain and force on time were realised by the test stand Andilog Stentor 1000. Certain mechanical parameters were determined, namely the diameter of the sample, length of the sample, force at 10% of strain, force in the first maximum of the force – strain curve, strain in the first maximum of the force – strain curve, modulus of elasticity, force in the inflex point of the force – time and force – strain curves and strain and stress in the

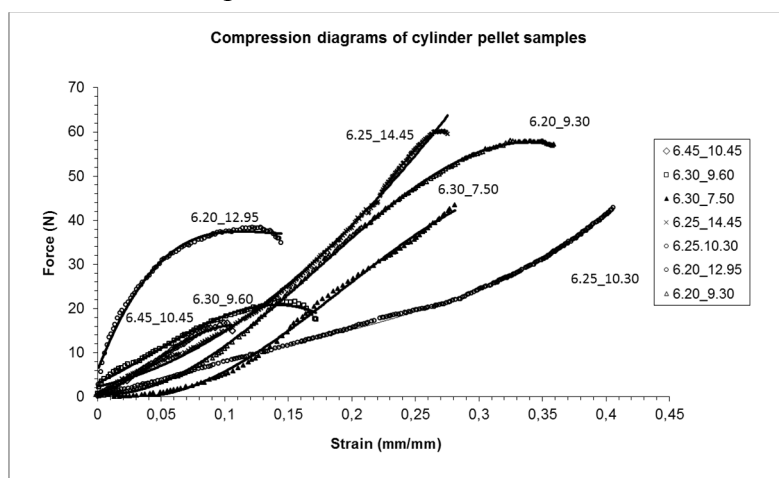


Fig. 1 Compression diagrams of the cylinder pellet samples as a dependence of force F (N) on strain ϵ (mm/mm).

Diameters d (mm) of the pellets are presented in the first column of the legend and lengths l_0 (mm) in the second column

presented in Fig. 1. The loading curves of different pellets had similar development, but the line shapes were different. There were influenced by the different lengths of the pellet samples. Compressive properties of the cylinder pellet samples are presented in Table 1. Characteristic point on the loading compressive curve in the compressing of the pellets between two metal plates was determined.

inflex point of the force – time and force – strain curves. Significant correlations of the mechanical parameters were observed between the inflex point and the first maximum point of the loading curves. There were find out, the compression force, stress and strain in the inflex point significantly correlate with the force, stress and strain in the first maximum. Compression diagrams of the cylinder pellet samples as dependence of force F (N) on strain ϵ (mm/mm) are

Table 1 Compressive properties of the cylinder pellet samples

n	d (mm)	l ₀ (mm)	F ₁₀ (N)	F _m (N)	ε _{mp} (mm/mm)	σ _{mp} (MPa)	ε _m (mm/mm)	σ _m (MPa)	E _e (MPa)	E (MPa)	F _{inf} (N)	ε _{inf} (mm/mm)	σ _{inf} (MPa)
1	6.45	10.45	16.49	16.69	0.10	0.51	0.10	0.46	5.29	5.05	7.50	0.05	0.22
2	6.20	9.30	10.81	57.91	0.33	1.99	0.33	1.29	8.16	7.86	28.52	0.17	0.78
3	6.25	10.30	7.99	18.08	0.24	0.62	0.29	0.57	2.58	2.57	12.58	0.16	0.34
4	6.25	14.45	14.99	59.90	0.27	1.96	0.34	1.24	7.80	5.99	41.70	0.21	1.07
5	6.30	7.50	5.04	57.46	0.33	1.24	0.34	1.24	7.49	6.90	23.98	0.19	0.64
6	6.30	9.60	17.99	21.62	0.15	0.70	0.15	0.59	4.38	2.37	11.63	0.05	0.35
7	6.20	12.95	37.44	38.34	0.13	1.27	0.12	1.12	7.03	7.03	37.34	0.10	1.12
Average	6.28	10.65	15.82	38.57	0.22	1.18	0.24	0.93	6.10	5.39	23.32	0.13	0.65
s	0.03	0.82	3.71	6.96	0.03	0.21	0.04	0.13	0.73	0.76	4.66	0.02	0.13
s (%)	0.48	7.68	23.47	18.04	15.07	18.14	15.81	13.97	11.92	14.16	19.98	17.82	19.54

d – original diameter of the sample; *l*₀ – original length of the sample; *F*₁₀ – force at 10% of the strain; *F*_m – force in the first maximum of the force – strain curve; ε_{mp} – strain in the first maximum determined from the force – strain curve; σ_{mp} – stress in the first maximum determined from the force – strain curve; ε_m – strain in the first maximum of the force – strain curve determined by calculation; σ_m – stress in the first maximum of the force – strain curve determined by calculation; *E*_e – modulus of elasticity determined from the slope of the linear part of the stress – strain curves; *E* – modulus of elasticity determined by calculation; *F*_{inf} – force in the inflex point determined from the force – time curve; ε_{inf} – strain in the inflex point determined by calculation; σ_{inf} – stress in the inflex point determined by calculation; *n* – number of sample; *s* – standard deviation

It is inflex point between the beginning of the loading curve and its first maximum. Compression force, stress and strain in the inflex point significantly correlating with the force, stress and strain in the first maximum were obtained. Measured values of mechanical parameters of the hay pellets are characterized by high dispersion. Two groups of compressive parameters characterized by positive and negative values of correlation coefficients were obtained. Diameter of the pellets and the initial firmness had negative correlation coefficients and their connection and influence on the next mechanical parameters were opposite. The initial firmness of the pellets determined by force at 10% deformation at strain 0.1 mm/mm did not influence on the total firmness of the pellet samples.

Acknowledgement

The research leading to these results has received funding from the European Community under project no 26220220180: Building Research Centre „AgroBioTech“.

Authors express the appreciations of the Scientific Grant Agency of the Ministry of Education of Slovak Republic and the Slovak Academy of Sciences within the framework of the research was realized in the project Biomaterials Physical Properties and Physical Methods Application for Specific Quality Indicators Assessment of Agricultural Materials no. 1/0854/14.

References

- [1] Hroncová E., Ladomerský J., The environmental and energy potential of incinerating various biomass mixtures. *Advanced Materials Research*, 2014, 1001, pp. 114–117.
- [2] Liu Z, Quek A, Balasubramanian R., Preparation and characterization of fuel pellets from woody biomass, agro-residues and their corresponding hydrochars. *Applied Energy*, 2014, 113, pp. 1315–1322.
- [3] Stelte W., Holm J.K., Sanadi A.R., Barsberg S., Ahrenfeldt J., Henriksen U.B., Fuel pellets from biomass: The importance of the pelletizing pressure and its dependency on the processing conditions. *Fuel*, 2011, 90, pp. 3285–3290.

Effect of ultrasonic pretreatment on biogas production potential from *Agropyron elongatum* biomass

Lalak J., Kasprzycka A., Tys J.

Institute of Agrophysics Polish Academy of Sciences, Doświadczalna 4, 20-290 Lublin, Poland

Corresponding author: j.lalak@ipan.lublin.pl

Keywords: Tall Wheat Grass, pretreatment, biogas, methane

Abstract

Agropyron elongatum 'BAMAR' (common name: Tall Wheat Grass) is a new energy crop with high renewability. It has recently been introduced to cultivation in Poland to provide biomass for bioenergy production. However, it presents a need for pretreatment to break down the lignin and to disrupt the crystalline structure of cellulose, so that enzymes can easily access and hydrolyze it (Kumar et al., 2009).

The biodegradability of the lignocellulose material can be increased by a pre-treatment. Many methods of pre-treatment have been studied. It can be carried out either physically, chemically or biologically, or as combinations of these. These methods are different from one another in terms of process efficiency, reaction conditions and complexity (Ramadoss and Muthukumar, 2016).

Ultrasound can be used as a pretreatment method for biomass. It is a physical technique that uses sound waves at ultrasonic frequencies (from 20 kHz to 10 MHz) (Oz and Uzun, 2015) to alter molecular structure of biomass. It has been extensively studied especially for sludge pretreatment before anaerobic processes to obtain better performance from anaerobic reactors by producing more bioavailable organic substrate and thereby facilitating the hydrolysis step. But it also has a disintegrating effect on the lignocellulosic structure and speeds up the hydrolysis – the limiting step of anaerobic digestion (Kwiatkowska et al., 2011; Bussemaker and Zhang, 2013).

This article analyses the impact of using ultrasound in the pretreatment of *Agropyron elongatum* 'Bamar' on the biogas production.

The research material was obtained from the Plant Breeding and Acclimatization Institute (IHAR) - National Research Institute, Radzików, Poland. The anaerobic inoculum used to carry out the AD-process was collected from a mesophilic biogas plant (Siedliszczki, Poland), which receives stillage (20%), corn silage (10%) and vegetable residue from the food industry (70%). It was incubated at 37°C for 5 days to decrease the background gas production. Prior to the start of the experiment, the inoculum was characterized by a volatile solids (VS) content of 3.86% (w/w) and pH of 7.8. The ultrasonic pretreatment was conducted using the laboratory sonication apparatus Vibra-Cell™ VCX500, Sonics generating waves of frequency 20 kHz. The parameters of ultrasonic pretreatment were as follows: reaction time 15, 30, 45 and 60 min, amplitude of ultrasonic waves 25%-100% of nominal output power (maximum). AD-process was carried out in a 2 liter Biostat B-plus stirred tank reactor (Sartorius Stedim Biotech, Gottingen, Germany). The temperature of the process was 37°C. Biogas production was measured and analyzed for methane content and methane yield. The process was conducted in three independent replicates till the moment when the daily yield of biogas was less than 1% of the total biogas yield obtained so far (DIN 38414/8). The values of biogas volume were converted to the normal conditions (1013 hPa, 273 K).

It could be shown, that ultrasound pretreatment of *Agropyron elongatum* for biogas production is technological and economical effective. The biogas yield and methane content could be increased up to 48% and 2.5 percentage points, respectively, whereas high reaction time and lower ultrasound amplitudes show the best results. The increased biogas yield could be

ascribed to increased bioavailability of biomass substrates. Furthermore, it was found that ultrasound pretreatment has an influence on the time of anaerobic digestion.

Integration of ultrasound pretreatment with anaerobic digestion process for *Agropyron elongatum* treatment could have a potential in obtaining a better performance and biogas amount with higher methane content. The methods can also be suitable to enhance anaerobic treatability of other energetic crops, especially ones in which hydrolysis rate is the limited step. Increase in anaerobic digestion rates can lead to lower retention times and smaller bioreactor volumes.

References

- [1] Bussemaker M. J., Zhang D., Effect of Ultrasound on Lignocellulosic Biomass as a Pretreatment for Biorefinery and Biofuel Applications. *Ind. Eng. Chem. Res.*, 2013, 52(10), pp. 3563–3580.
- [2] Kumar P., Barrett D. M., Delwiche M. J., Stroeve P., Methods for pretreatment of lignocellulosic biomass for efficient hydrolysis and biofuel production. *Ind. Eng. Chem. Research*, 2009, 48, pp. 3713–3729.
- [3] Kwiatkowska B., Bennett J., Akunna J., Walker G. M., Bremmer D. H., Stimulation of bioprocesses by ultrasound, *Biotechnol. Adv.*, 2011, 29, pp. 768–778.
- [4] Oz N. A., Uzun A. C., Ultrasound pretreatment for enhanced biogas production from olive mill wastewater. *Ultrason. Sonochem.*, 2015, 22, pp. 565–572.
- [5] Ramadoss G., Muthukumar K., Mechanistic study on ultrasound assisted pretreatment of sugarcane bagasse using metal salt with hydrogen peroxide for bioethanol production. *Ultrason. Sonochem.*, 2016, 28, pp. 207-217.

Methodology for testing the accuracy of GPS autonomous UAVs as perimeter protection

Lešetický J.

Czech University of Life Sciences Prague, Kamýcká 129, 16521 Prague 6, Czech Republic

Corresponding author: Lešetický J., e-mail: leseticky@tf.czu.cz

Keywords: UAV, GPS, Methodology

Abstract

This method is created on the basis of contract research under a contract dated 14.3.2016.

Testing will be done on the initiative of CAA simplify the approval of licenses for commercial use under legal conditions. After analyzing the results, it is also considered the possibility of transmission line UAV GPS coordinates to maps for monitoring their position.

An important factor for the commercial use of autonomous UAV in various sectors is correct authentication navigation elements. The main reason for this test is a potential risk of failure or possible inaccuracies high navigation system, which could result in damage to both airspace, and persons or property on the ground. Conflict unprotected adult or even a child with a rotating propeller could cause very serious or even fatal injuries.

GPS is used as a component of the safety system "failsafe" and variant "Go home." In case of failure or loss of control signal directs flown along the trajectory of UAV to return to the starting point. Then it is part of "geofencing" that prevents bezpilotnímu means fly into a restricted area. Once the UAV approaches to this area, it is automatically changed to the direction of flight so as to go around the bordered space.

To determine the performance parameters of the GPS receiver will initially selected basic static measurements. For this method, you must antenna GPS device placed on a point with known coordinates national coordinate system with pre-verified as accurate. Measurements will be made after a predefined period of time, under different weather conditions and at several different locations in the range of PDOP (Position Dilution Of Precision), to the value of 4.0, which corresponds to about 90% of the time of day (see Tab. 1). When shooting must be taken into account the possibility of shading signal silhouette, and therefore there is approximation only for the time necessary to change the parameters of shooting positions. Table of the measurement will be completed on time, weather conditions (temperature, cloudiness, precipitation and strange atmospheric phenomena), DOP values, the configuration of the satellites (skyplot - important in places with poor visibility of the sky) and the orientation of the device to the cardinal [1], [2], [3].

Tab. 1 Table of PDOP values

PDOP	Description
= 1	Ideal state - impossible
≤ 4	Very precise value
≤ 8	Upper limit of the applicability of the results
≤ 20	Unusable values

Furthermore, the GPS device UAV subjected to a dynamic measurement, which will record data in motion. The movement is designed in the shape of polygons (Fig. 1), which are most often shaped such as parcels or the occurrence of game. For the measurement will be elected polygon circumscribing the runway, which will mean a test sample restricted area and that will also be



Fig. 1: Demonstration of a polygon flight path

tested as well as "geofencing" system. Other proposed polygons will also go through areas with different observational conditions, slope, valley. The purpose of this measurement is to determine and evaluate how the GPS receiver on a UAV behaves in different conditions at different speeds with respect to current and legislative conditions. This means that the UAV will be exposed to real-world conditions, which may deteriorate the conditions of the GPS signal. This mode will record the GPS coordinates of the intervals of 1s. Table of the measurement will be completed on time, weather conditions (temperature, cloudiness, precipitation and strange atmospheric phenomena), DOP values, the configuration of the satellites (skyplot - important in places with poor visibility of the sky) and the orientation of the device to the direction of flight [1], [2],[3].

Recorded are the two methods of measurement will be plotted on maps and displays.

Subsequently, statistically analyzed and evaluated. When creating this method for testing the accuracy of GPS UAV was necessary to take into account that the autonomous flight will be carried out in accordance with current legislation.

Acknowledgement

The work is supported by the research project for KELCOM company.

References

- [1] Chosa T., Omine M., Itani K., Ehsani R., Evaluation of the Dynamic Accuracy of a GPS Receiver, Eng. Agric. Environ. Food, 2011, pp. 54–61.
- [2] Dogan U., Uludag M., Demir D., Investigation of GPS positioning accuracy during the seasonal variation, Measurement, 2014, pp. 91–100.
- [3] Vaniš P., Kocáb M., Testování aparatur GPS pro navigační systémy a mobilní sběr geodat. 1st International Trade Fair of Geodesy, Cartography, Navigation and Geoinformatics GEOS (2006): 62.

Influence of temperature on power of photovoltaic modules

Malínek M., Božíková M., Hlaváč P., Cviklovič V., Olejár M., Pavlovič S.
Slovak university of agriculture in Nitra, Tr. A. Hlinku 2, 94976 Nitra, Slovak Republic

Corresponding author: Božíková M., e-mail: Monika.Bozikova@uniag.sk

Keywords: photovoltaic modul, power, solar energy, temperature

Abstract

Photovoltaic conversion of electromagnetic radiation to electric power takes place in semiconductor photovoltaic (PV) cells [1]. In this contribution are presented photovoltaic system components and results of measurements which were made during one year period.

In our case, experiments were carried out on two photovoltaic systems in the wiring grid-on. The power of photovoltaic system was 29 kW. Both solar systems were located in village Česká in Czech Republic. Photovoltaic system consist from photovoltaic modules EGM – 220 with maximum electric power 220 W. Photovoltaic panels are connected to produce required electric voltage and electric current for power inverters Fronius IG 150. Peak power of photovoltaic system is 29 kWp. Produced electric power is monitored and recorded by device Fronius Dataloger Web. Photovoltaic modules EGM 220 are connected, but they are divided into two parts. The first part is marked as IG-A and the second part is marked as IG-B. The PV modules IG-A had azimuth 190° from the south and the angle of PV module inclination was 35° from the horizontal plane. The orientation of PV modules IG-B was 240° from the south and angle of inclination was 30°.

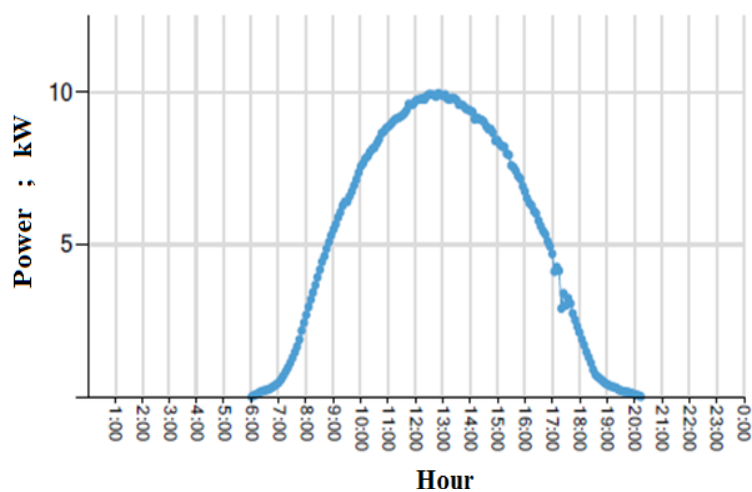


Fig. 1 Power characteristic measured summer day

There was measured energy produced by photovoltaic module in every month during one year period for photovoltaic modules IG-A and IG-B and were obtained power characteristic as relation of power to time for every day. The power characteristics for selected days are presented on Fig. 1 and Fig. 2. The first graphical relation – Fig. 1 presents power of PV modules for ideal sunny day in August. Measurement of electric power started in the morning at the sunrise (5 h 56 min) and finished at the sunset (20 h 20 min). Electric

power was recorded in 5 minutes time intervals. Day power was calculated as sum of all measured power values. The second graphical relation – Fig. 2 was obtained for typical winter day in January. The measurement of power characteristic started in the morning at the sunrise (7 h 58 min) and finished at sunset (16 h 05 min). Low values of produced power were caused by changeable and cloudy weather.

The minimal values of produced energy were obtained for winter months and maximal values for summer months. From daily measurements of energy production is clear, that solar irradiation changes during the day.

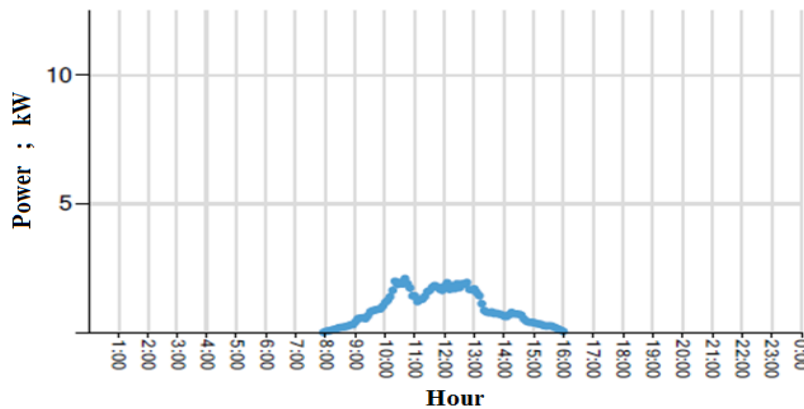


Fig. 2 Power characteristic measured during winter day

optimal temperature of photovoltaic cell surfaces [2], which was higher than temperature of photovoltaic modules IG-B. Worse orientation of photovoltaic

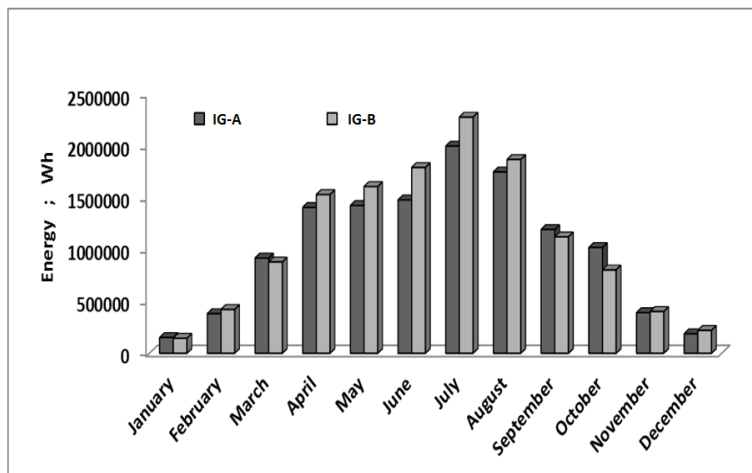


Fig. 3 Comparison of energy produced by photovoltaic modules during one year period

In sunny day solar irradiation culminate at 12:00 hour (Fig. 1). From results obtained for every month (from January to December) were detected differences between theory and practise, which are evident from results presented on Fig. 3. Better oriented photovoltaic modules IG-A had lower energy production during five months.

This fact was caused by no optimal temperature of photovoltaic cell surfaces [2], which was higher than temperature of photovoltaic modules IG-B. Worse orientation of photovoltaic modules IG-A to the south had negative influence on module surfaces irradiation by the sun light, so the surfaces of photovoltaic modules IG-B had lower temperature which was nearer to the optimal semiconductor working temperature. It was the main reason of higher values of electric energy production by modules IG-B. The PV modules with better orientation had higher temperature and their temperature was out from optimal working temperature range of semiconductors.

There were detected differences between theory and practise during the measurements. In theory presented ideal south orientation of solar irradiated surfaces does not mean optimal working condition for photovoltaic cells which were made from semiconductors. The measurements of photovoltaic modules power in real conditions demonstrated that temperature is one of the most important factors that affect their power characteristics.

References

- [1] Poulek V., Libra M., Photovoltaics, theory and practice of solar energy utilization, ILSA, Prague, 2010, 169 pages, ISBN 978-80-904311-2-6.
- [2] Cviklovič V., Olejár M. Temperature dependence of photovoltaic cells efficiency. Trends in Agricultural Engineering 2013. 1st. Ed. Prague : Czech University of Life Sciences Prague, 725 pages, ISBN 978-80-213-2388-9.

Experience Gathered with the unique Photovoltaic Power Plant in Central Part of Historical City

Olšan T.¹, Libra M.¹, Poulek V.¹, Avramov V.²

¹ Czech University of Life Sciences Prague, Kamýcká 129, 16521 Prague 6, Czech Republic

² ENESA, joint-stock company, Prague, Czech Republic

Corresponding author: Olšan T., e-mail: tolsan@email.cz

Keywords: photovoltaics, flexible PV panels, power plant.

Abstract

The unique photovoltaic (PV) power plant installed in Prague on the roof of the new buildings of National Theatre in Prague has been constructed and monitored. The location is in the historical city centre. Also the power plant must to be totally invisible from the streets to not disturb historical panorama of the city. Flexible a-Si photovoltaic foils in the nearly horizontal position have been used. The operation started in the autumn 2009. The photovoltaic power plant is described in this paper and six years experience of its operation is presented. The energy production data indicate that the degradation of the nearly horizontally installed a-Si panels is below 5% within 6 years period.

Importance of the energy efficient building increases especially because of the increasing availability of the renewable energy sources. Different types of PV panels and PV arrays were described for instance in next reports [1-4].

We consider the reconstruction of the National Theatre roof with the incorporated PV power plant a suitable solution as the theatre management behaves ecologically. Regardless of the fact that the PV power plant described above can cover only a small part of the power consumption of the theatre, the roof is purposefully used. The PV power plant construction on the basis of flexible PV foils was the only acceptable alternative with respect to the Prague historical center conservation requirements. The PV power plant is not visible and the view on the Neo-Renaissance building of the National Theatre is not distracted as well as the view on the New Scene Building and Service Building.

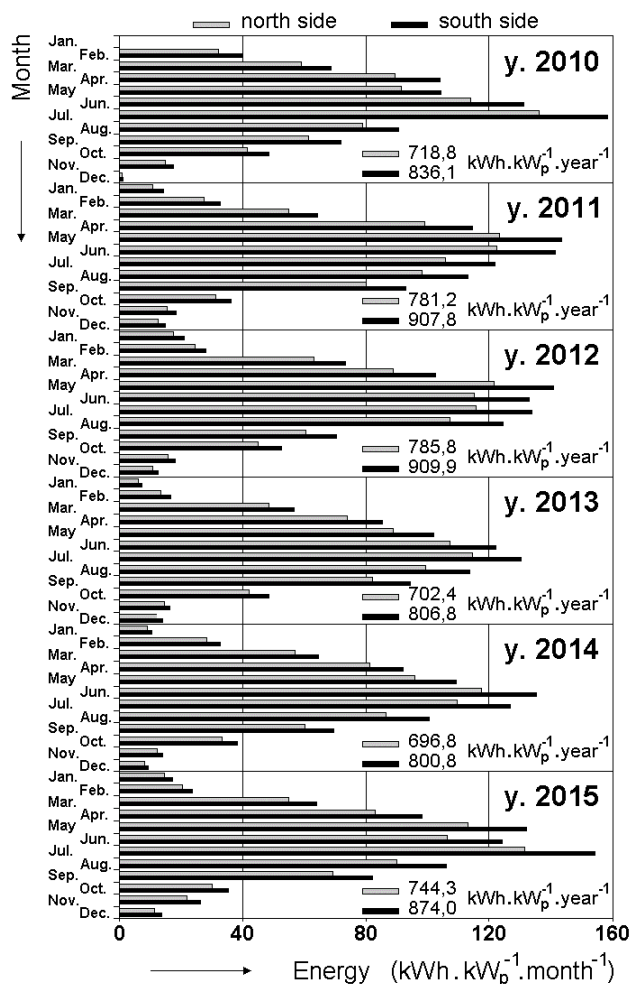


Fig. 1 Electric energy produced in the PV power plant on the National Theatre New Scene Building roof during the years 2010-2014.

view on the New Scene Building and Service Building.

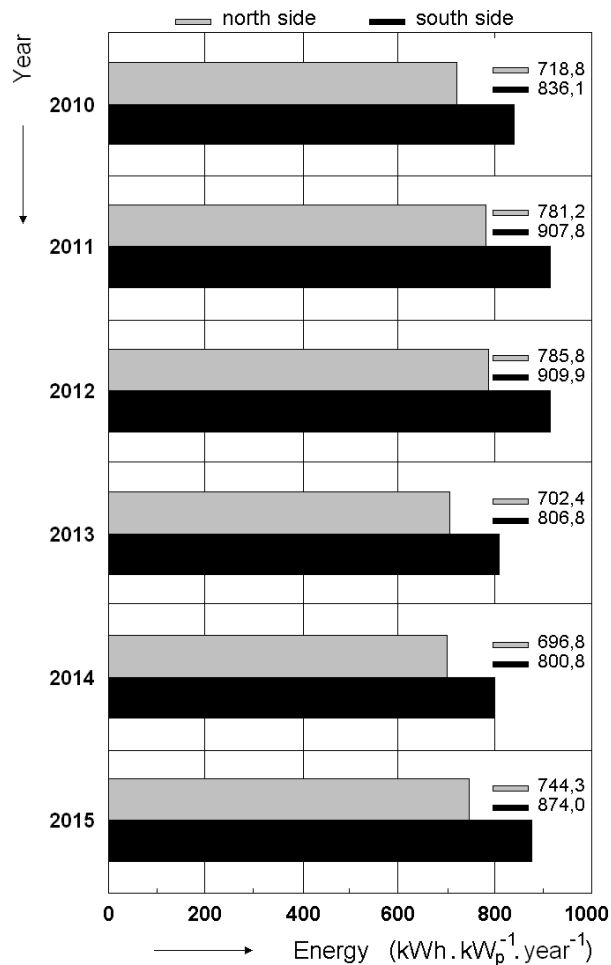


Fig. 2 The annual energy production during the years 2010÷2015

The energy production within the 6 years period is better than expected (see Figs. 1, 2). The energy production degradation is ranging from 3÷4%. It is low value for a-Si thin film panels laminated in polymer foils. The typical degradation value is about 5%. Additionally, the panels are installed with very low tilt angle 3 degrees only. The polluted air in the center of big city is contributing to substantial soiling of the panels. So the soiling loss alone can contribute to 2÷3% of the degradation. These results indicate that a-Si PV panels laminated in plastic film can have low degradation of the energy production even if it is installed horizontally in polluted urban environment.

Although the difference between the angles of the both sides of the PV system is 6° only, the annual energy production difference is approx. 15%.

We intend to continue in the collection of data and it will be certainly interesting to observe how the measured values will change in connection with the whole construction ageing. The lifetime of the PV panels was simulated in [5]. The comparison with our collected data will be interesting. These data will be of interest also for designers of other roof PV systems.

References

- [1] Matuška T., et al., Glazed PVT Collector with Polysiloxane Encapsulation of PV Cells: Performance and Economic Analysis. *International Journal of Photoenergy*, 2015, Article ID 718316.
- [2] Libra M., et al., Comparison of photovoltaic power plants of various design and location in the Czech Republic. *Fine Mechanics and Optics*, 2011, 56, 5, pp.156-159 (in Czech).
- [3] Cerón, J.F., et al., A coupled numerical model for tube-on-sheet flat-plate solar liquid collectors. Analysis and validation of the heat transfer mechanisms. *Applied Energy*, 2015, 142, pp.275–287.
- [4] Crisostomo, F., et al., Spectral splitting strategy and optical model for the development of a concentrating hybrid PV/T collector. *Applied Energy*, 2015, 141, pp.238–246.
- [5] Hasan, O., Arif, A.F.M., Performance and life prediction model for photovoltaic modules: Effect of encapsulant constitutive behavior. *Solar Energy Materials and Solar Cells*, 2014, 122, pp.75-87.

Loop-mediated isothermal amplification (LAMP) for detection of *Talaromyces flavus*

Panek J., Frać M.

Institute of Agrophysics Polish Academy of Sciences, Doświadczalna 4, 20-290 Lublin, Poland

Corresponding author: Panek J., e-mail: j.panek@ipan.lublin.pl

Keywords: LAMP, Loop-mediated isothermal amplification, heat-resistant fungi, *Talaromyces flavus*

Abstract

Talaromyces flavus is heat-resistant fungus able to survive heat-treatment during process of pasteurization and is responsible for spoilage of heat-processed food [1, 2]. *T. flavus* displays ability to produce numerous mycotoxins, and therefore presents serious threat to food safety [3]. To minimize impact of *T. flavus* on food spoilage, there emerge need of rapid and sensitive detection of this fungus in samples. Detection of *T. flavus* is conducted by usage either of traditional plate or microscopic techniques or by usage of methods based on molecular biology. Techniques based on polymerase chain reaction (PCR) are both faster and more sensitive than traditional plates. However, they require expensive laboratory equipment such as thermocyclers. Development of Loop-mediated isothermal amplification (LAMP) technique seems to be a solution for this problem [4]. LAMP is also reported to be faster and more sensitive reaction than PCR [5].

LAMP is a method of DNA isothermal amplification. Technique is based on use of four or six primers complimentary to six or eight gene regions. Double stranded DNA at the temperature about 60-65°C is in the condition of dynamic equilibrium, which allows the annealing of complimentary primers without the need of DNA heat denaturation. After that, LAMP utilizes the properties of DNA polymerase with strand displacement activity and starts amplification. LAMP allows observing positive reaction in about 30 minutes.

The aim of this study was the development of specific, sensitive and rapid LAMP method for detection of *Talaromyces flavus*. Specificity of designed primers was tested by performing reaction with 5 *Talaromyces flavus* reference isolates and 14 isolates of other fungi species. We performed the DNA extraction with column-based procedure [6]. We designed three pairs of LAMP primers – Tf_F3, Tf_B3, Tf_FIP, Tf_BIP, Tf_LoopF and Tf_LoopB. We used Isothermal MasterMix (OptiGene) with dsDNA binding 6-FAM based dye. We optimized all the crucial conditions of LAMP reaction, such as primers concentration, MasterMix concentration, reaction volume or reaction time. The sensitivity of method was tested with DNA of concentration ranging from 1fg to 10ng of genomic DNA. Results of this step were compared to sensitivity of traditional PCR reaction with Tf_F3 Tf_B3 primers. The results of reaction were visualized with electrophoresis on agarose gel (2%, 7V/cm). LAMP reaction kinetics was visualized by measurement of fluorescence every 60 second of reaction in real-time PCR thermocycler (Applied Biosystems 7500 Fast).

Designed and optimized LAMP reaction was successful in whole range of studied DNA concentrations – 1fg to 10ng, where traditional PCR reaction was positive only in concentrations higher or equal 1pg of genomic DNA as presented at Fig. 1. We observed positive results of reaction in 35 minutes for DNA concentration from 10fg to 10ng and in 55 minutes for 1fg of genomic DNA.

Proposed LAMP technique is very sensitive, rapid and cost effective method for detection of *Talaromyces flavus*.

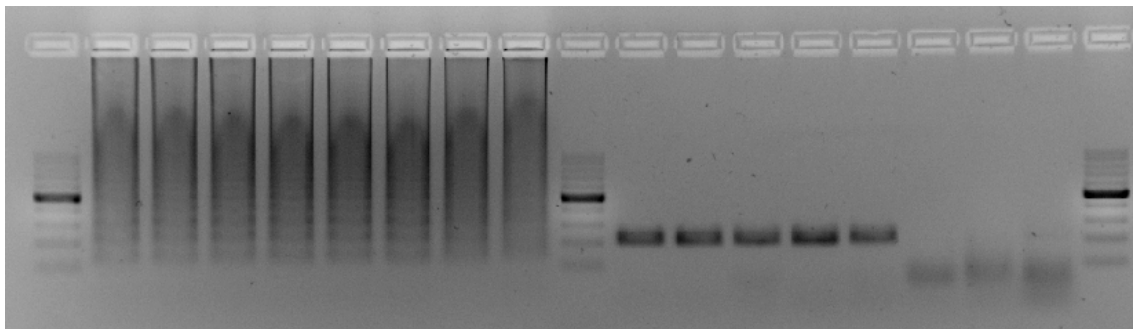


Fig. 1 Comparison of detection sensitivity of LAMP and PCR reactions. Amplicons obtained with (from left to right) 10ng, 1ng, 100pg, 10pg, 1pg, 100fg, 10fg and 1fg of *Talaromyces flavus* genomic DNA

Acknowledgement

The research is funded by the Polish Ministry of Science and Higher Education under the Diamond Grant program, project No.: 0204/DIA/2013/42

References

- [1] Jesenská Z., Piecková E., Bernát, D., 1993. Heat resistance of fungi from soil. *International Journal of Food Microbiology*, 19, pp. 187-192.
- [2] Samson R.A., Yilmaz N., Houbraken J., Spierenburg H., Seifert K.A., Peterson S.W., Varga J., Frisvad J.C., 2011. Phylogeny and nomenclature of the genus *Talaromyces* and taxa accommodated in *Penicillium* subgenus *Biverticillium*. *Studies in Mycology*, 70, pp. 159-183.
- [3] Proksa B., 2010. *Talaromyces flavus* and its metabolites. *Chemical Papers*, 64, pp. 696-714.
- [4] Notomi T., Okayama H., Masubuchi H., Yonekawa T., Watanabe K., Amino N., Hase T. 2000. Loop-mediated isothermal amplification of DNA. *Nucleic Acid Research* 28, 12, p. 63.
- [5] Ptaszyńska A. A., Borsuk G., Woźniakowski G., Gnat S., Małek, W. 2014. Loop-mediated isothermal amplification (LAMP) assays for rapid detection and differentiation of *Nosema apis* and *N. ceranae* in honeybees. *FEMS Microbiol Lett* 357, 1, pp. 40-48.
- [6] Panek J., Frać M. 2015. Evaluation and optimization of DNA extraction procedures for *Talaromyces flavus*. 14th International Workshop for Young Scientists, BioPhys Spring 2015 Gödöllő, Hungary, 27-29.05.2015, 2015, pp. 46-47.

Electrical Properties of Perga

Regrut T., Hlaváčová Z., Petrovič A., Csillag J.

Slovak University of Agriculture in Nitra, Tr. A. Hlinku 2, SK-949 76 Nitra, Slovakia

Corresponding author: Regrut T., e-mail: tregrut@gmail.com

Keywords: perga, electrical properties, capacitance, resistivity

Abstract

The dielectric properties of foods and biological products have become valuable parameters in food engineering and technology. The investigation material and moisture measurement using electromagnetic waves in wide spectrum serve for quality control and improvement in many branches like industry, forest and wood-working industry, civil engineering, agriculture, commerce and also foods e. g. for quality evaluation of meat, fruits, coffee etc., [1] and [2].

Measurement of electrical properties is one of the most important operations in the collection, storage and processing of the agricultural production. The physical properties of biological materials affect measurement accuracy. These properties are in a very difficult relationship between them. Biological materials are macroscopic and microscopic considerably inhomogeneous. They have a non-homogeneous chemical structure, have different densities, and containing also contaminants. Moreover, many of them develop a continuous biological activity.

Bee bread - also called "Perga"- are fermented bees pollen in the comb, which store bees as protein supply. The bee bread is harvested by hand from the honeycomb and thus is not only the most valuable, but also the most expensive bee products [3]. Bee bread is considered the most perfect of all natural foods - used by the Greeks as ambrosia. It includes many vitamins (A, B₁, B₂, B₆, B₁₂, C, D, E, P, PP) and trace elements (potassium, magnesium, calcium, copper, iron, silicon, sulphur, chlorine, manganese) [3]. In the perga there is everything that is required for the normal growth and existence of a live organism. Good results are noted by specialists at treatment of patients with many diseases [4].

We obtained the sample of perga from the Faculty of Agrobiolgy and Food Resources of SUA in Nitra. We were made the initial measurement of physical properties. The sample was placed in the sensor with parameters: diameter of electrode 37.8 mm, electrodes spacing 49.2 mm, mass of empty sensor 208.89 g. Electrical properties of perga were measured by an instrument GoodWill Instek LCR meter 821 at different frequencies using four-electrode (tetra polar) system. We measured several electrical properties, such as capacitance, resistance, impedance and loss factor. Each property was measured in the frequency range from 0.1 kHz to 200 kHz, at all frequencies three times. Average value and standard deviation has been computed from these ones. The measured values were loaded by PC.

For example, the values of resistance were in Tab. 1.

Tab. 1 The values of resistance at frequency of 1 kHz

Number	Resistance R (k Ω)	Δ_+ (k Ω)	Δ_- (k Ω)
1	160.01		0,04
2	159.96	0.01	
3	159.94	0.03	
Average	159.97		

The standard deviation of this measurement was 0.0208 kΩ. And also in other cases has the standard deviation very small value. From measured and calculated values are constructed graphical dependencies of electrical quantities on frequency. For illustration, the resistance and impedance versus frequency curves are shown on Fig. 1.

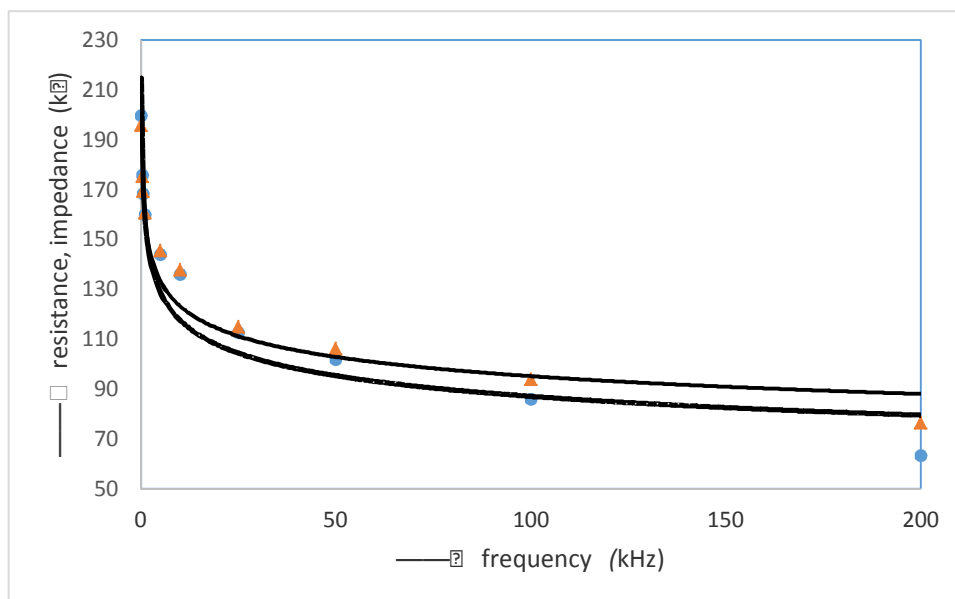


Fig. 1 The resistance ● and impedance ▲ versus frequency curves

The regression equation for resistance and impedance has the shape of decreasing power function

$$R = R_0 \left(\frac{f}{f_0} \right)^{-k}$$

where: R – resistance, $R_0 = 158.98$ kΩ – reference resistance, f – frequency, $f_0 = 1$ kHz, $k = 0.131$ – constant. The similar equation can be write also for impedance. The coefficient of determination has high value $R^2 = 0.9089$. The impedance has a slightly higher values as resistance, which is caused by the capacitance of perga. Also the capacitance decreases with frequency according to power function. Only loss factor increased in this frequency range.

Acknowledgement

This work was supported by research project VEGA 1/0854/14 of Ministry of Education, Science, Research, and Sport of the Slovakia and was co-funded by the European Community under the project No 26220220180: Building the Research Centre AgroBioTech.

References

- [1] Hlaváčová Z., Low Frequency Electric Properties Utilization in Agriculture and Food Treatment. RES. AGR. ENG., 2003, 49, 4, p. 125-136.
- [2] Venkatesh M. S., Raghavan, G. S. V., An Overview of Dielectric Properties Measuring Techniques. Canadian Biosystems Engineering, 2005, 47, p. 7.15-7.30.
- [3] McIntyre P., Snyder A. W., Light Propagation in Twisted Anisotropic Media: Application to Photoreceptors. Journal of the Optical Society of America, 1978, 68, 2, p. 149-157.
- [4] Georgiev D. B., Goudev, A. G., Manassiev N., Effects of an Herbal Medication Containing Bee Products on Menopausal Symptoms and Cardiovascular Risk Markers: Results of a Pilot Open-uncontrolled Trial. MedGenMed, 2004, 6, 4, 46, 12 pp. <http://www.ncbi.nlm.nih.gov/pmc/articles/PMC1480585/>

The effect of supplementary red and blue light on the growth of lettuce under white fluorescent lamps

Siecińska J., Nosalewicz A.

Institute of Agrophysics Polish Academy of Sciences, Doświadczalna 4, 20-290 Lublin, Poland

Corresponding author: Siecińska J., j.wrobel@ipan.lublin.pl

Keywords: Light Emitting Diodes (LED), lettuce, supplementary light, red and blue light

Abstract

Studies on the application of light-emitting diodes (LEDs) in plant culture systems have been conducted for over 20 years. Light-emitting diodes (LEDs) have tremendous potential as supplemental or sole-source lighting systems for crop production both on and off earth. Their small size, durability, long lifetime, cool emitting temperature, and the option to select specific wavelengths for a targeted plant response make LEDs more suitable for plant-based uses than many other light sources. These advantages, coupled with new developments in wavelength availability, light output, and energy conversion efficiency, place us on the brink of a revolution in horticultural lighting.

The aim of the study was to evaluate the effect of supplementation of fluorescent lights with red and blue LEDs on the rate of lettuce growth, photosynthesis, colour and biomass.

The lettuce (*Lactuca sativa*) were grown in 7.5 cm in diameter and 10 cm height soil columns filled with garden soil (Kronen, Poland). Conditions during plant growth under fluorescent lights (FL) were as follow: temperature of the day and night 24°C (9h) / 18°C (15h), light intensity 80 $\mu\text{mol m}^{-2}\text{s}^{-1}$ (PAR) under white fluorescent lights (Philips Master 80W 840), relative air humidity 60%. The conditions during lettuce growth under supplementary red and blue light emitting diodes (FL+LED) were as under FL but additional light source were LED lamps (OSRAM, PP Electronix, Poland). LED lamps were used for 5 hours in the morning and 3h in the evening. Before switching on hours in the morning and 3 in the evening am to 10 am and from 2 pm to 5 pm to extend day period, light intensity as summaries of fluorescent and LED 108 $\mu\text{mol m}^{-2}\text{s}^{-1}$.

The used red and blue LEDs exhibit two narrow bands in the blue and red spectral regions with maxima at - 451 and 640 nm, respectively the ratio of red to blue was 6:2.

The measurements included leaf gas exchange, chlorophyll content and leaf reflectance. During the harvest day (20th day from sowing) fresh and dry weight of leaves were measured.

The measurements of photosynthesis rate and transpiration from the leaf was measured by the system of gas exchange unit GFS 3000 (Walz, GmbH) at light intensity at 100, 200, 400, 800 and 1600 $\mu\text{mol m}^{-2}\text{s}^{-1}$. The measurements was conducted in 8 cm² cuvette, the conditions in the cuvette were on the same level as in the growth room: air temperature 24°C, relative humidity 60%, CO₂ concentration 400 ppm.

The leaf chlorophyll content was measured using a chlorophyll content meter CCM-300 (Opti-Science, USA). The measurements of leaf reflectance was measured by the Miniature Leaf Spectrometer CI-710 (Bio-Science, USA). Measurements were taken from the adaxial leaf surface. From the data obtained, average percentage reflectance over the 400–1000 nm range was determined. Reflectance measurements are used to derive the PRI (Physiological Reflectance Index), NDVI (Normalised Difference Vegetation Index) and NPQI (Normalised Phaeophytinization Index) spectral indices.

Our results demonstrated that the supplementation of lettuce growth with LED light greatly influences its rate of growth. The Figure 1 portrays the visual comparisons, the dramatic difference in plant size is clearly observed.



Fig.1. Lettuce grown for 15 days under sole fluorescent (left) light source and under fluorescent and supplementary LED light source (right).

The highest content of chlorophyll was found in the treatment FL+LED. These and other results [2] confirm that leaves under red plus blue LEDs contain more chlorophyll and carotenoids in comparison to other treatments. During the experiment photosynthesis intensity, stomatal conductance of CO₂ and transpiration of lettuce leaves were higher in FL+LED (with LED light supplementation) than in FL (without LED light supplementation) under all light intensities. This could be a result of adaptation to higher light intensities which stimulates photosynthesis in plants [4] and higher

chlorophyll content. A clear stimulation of photosynthesis intensity during supplemental lighting with the LEDs in this experiment resulted in rosettes with the higher weight. The mean rosette fresh weight was 22 g as compared to only 0.98 g in treatment without LED light. The changes in spectral reflectance indices are observed between variants. In the treatment FL the PRI values are higher in comparison to the values of FL+LED treatment as a result of chlorophyll degradation and simultaneous increase in the carotenoid to chlorophyll ratio. The results of this study are promising, whether further research is needed to evaluate potential of LED light supplementation in horticulture.

References:

- [1] Hogewoning S.W., Trouwborst G., Maljaars H., Poorter H., van Leperen W., Harbinson J., Blue light dose-responses of leaf photosynthesis, morphology, and chemical composition of *Cucumis sativus* grown under different combinations of red and blue light. *J. Exp. Botany*, 2010, 61(11), pp. 3107-3117.
- [2] Shin K.S., Murthy H.N., Heo J.W., Hahn E.J., Paek K.Y., The effect of light quality on the growth and development of in vitro cultured *Doritaenopsis* plants. *Acta Physiol. Plant.*, 2008, 30, pp. 339-343.
- [3] Trotter G.M., Whitehead D., Pinkney E. J., 2002. The photochemical reflectance index as a measure of photosynthetic light use efficiency for plants with varying foliar nitrogen contents. *Int. J. Remote Sensing*, 2002, 23(6), pp. 1207–1212.
- [4] Wang H., Gu M., Ciu J., Shi K., Zhou Y., Yu J., Effects of light on CO₂ assimilation, chlorophyll quenching, expression of Calvin cycle genes and carbohydrate accumulation in *Cucumis sativus*. *J.Photochem. Photobiol. B: Biology*, 2009, 96, pp. 30-37.

Detection of gray mold infection using hyperspectral reflectance imaging

Siedliska A., Baranowski P.

Institute of Agrophysics Polish Academy of Sciences, Doświadczalna 4, 20-290 Lublin, Poland

Corresponding author: Siedliska A., e-mail: a.siedliska@ipan.lublin.pl

Keywords: strawberries, hyperspectral imaging, gray mold

Abstract

Strawberry fruits are one of the most popular berry fruits in the world. They are characterized by a short postharvest life. Due to their chemical composition and delicate surface texture they are highly perishable and vulnerable to tissue damage during harvest and postharvest handling and storage [4]. One of the most serious and common fruit diseases of strawberries is gray mold, which is caused by the fungus *Botrytis cinerea* [1]. It is really difficult to control gray mold, because that pathogen can infect all plant parts, mostly during the ripening and at harvest. *Botrytis cinerea* is especially hazardous as a postharvest pathogen because in packing unit the fungal infection can spread to adjacent healthy strawberries, causing losses during shipping and marketing [2]. The spectroscopic and imaging techniques are unique monitoring methods that have been used to detect diseases in plants as well as mechanical injuries such as bruises [3]. The objective of this research was to determine the efficiency of visible and near infrared hyperspectral imaging technique to detect physicochemical changes in strawberries fruit after infection of *Botrytis cinerea* fungi.

The experimental samples were 'Senga Sengana' strawberries, hand harvested in the local farm located in Lubelskie region. Strawberries were divided into two groups: one was kept as control (non inoculated), while the second was inoculated by spraying *Botrytis cinerea* conidial suspension. The strawberry fruits were stored at 20°C and 85% relative air humidity. In total 200 inoculated and non inoculated fruits were tested by a hyperspectral imaging setup working in the visible and near-infrared (400-1000 nm) wavelength range. In order to assess the real quality parameters of fruit (soluble solid content, dry mass content, firmness, phenolic and anthocyanin content) were determined using destructive tests. Hyperspectral measurements and standard quality tests were performed during the period of four days until the visual changes were observed.

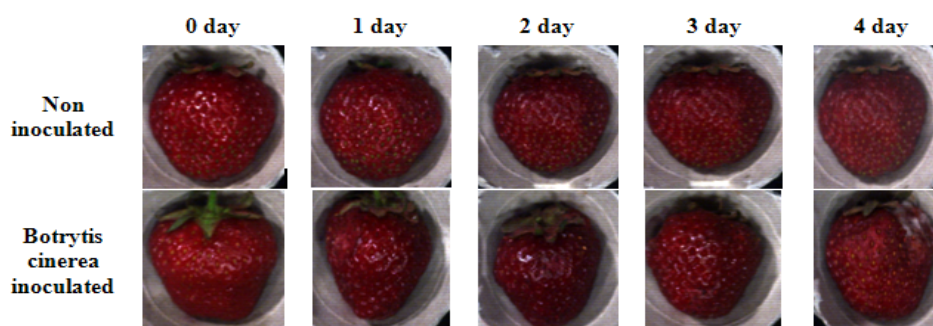


Fig.1 RGB hyperspectral images of artificially infected with *Botrytis cinerea* strawberry fruits

The representative RGB hyperspectral reflectance images of inoculated and non inoculated strawberries are presented in Figure 1. It can be noticed that visual symptoms of gray mold occurred at 4th day after inoculation (all the infected fruits had characteristic gray spots).

Figure 2 shows a comparison of the mean reflectance spectra of the strawberry fruits on various days after inoculation by *Botrytis cinerea* fungi and non inoculated fruits with shaded error bar, representing standard deviations for all control measurements (four days). The significant differences between spectral characteristics of inoculated and non inoculated fruits were observed throughout the whole spectral range. Infected fruits showed lower spectral reflectance than healthy fruits, even when symptoms are still not visible.

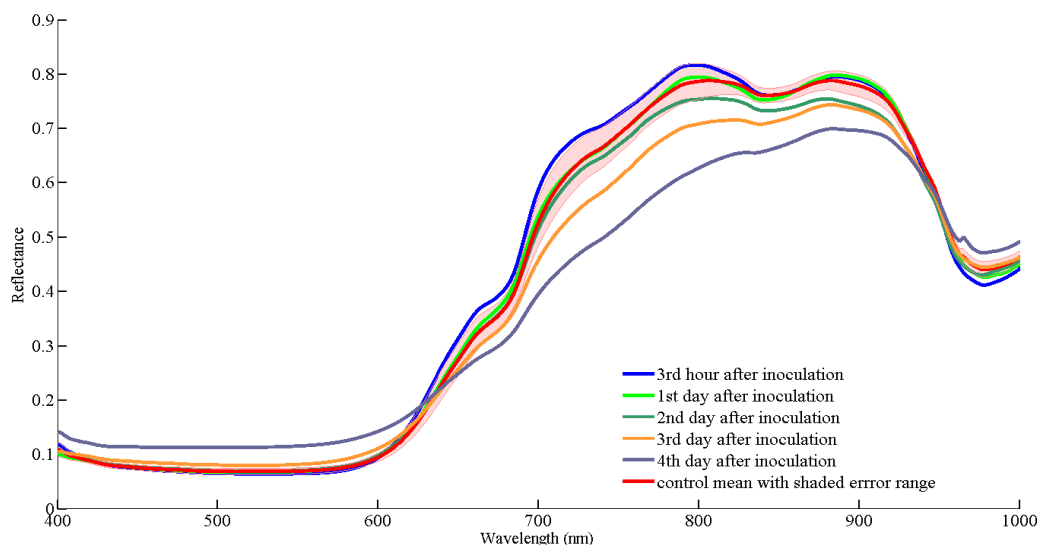


Fig. 2 Spectral characteristics of infected and non infected strawberry fruits during four days storage

The results obtained using hyperspectral imaging system was used to develop classification models for identification gray mold in strawberry fruits. The pretreatment method consists of second derivative transformation of the spectral data. The best classification accuracy (82% of correctly classified instances) was achieved by SVM model using 29 selected wavelengths.

This research proved that the different infection stages of strawberry gray mold can be identified through hyperspectral imaging analysis.

References

- [1] Freeman, S., Minz D., Kolesnik I., Barbul O., Zveibil A., Maymon M., Dag A., Trichoderma biocontrol of *Colletotrichum acutatum* and *Botrytis cinerea* and survival in strawberry. *European Journal of Plant Pathology*, 2004, 110(4), pp.361-370.
- [2] Pan L., Zhang W., Zhu N., Mao S., Tu K., Early detection and classification of pathogenic fungal disease in post-harvest strawberry fruit by electronic nose and gas chromatography–mass spectrometry. *Food Research International*, 2014, 62, pp.162-168.
- [3] Siedliska A., Baranowski P., Mazurek W., Classification models of bruise and cultivar detection on the basis of hyperspectral imaging data. *Comput. Electron. Agric.*, 2014, 106, pp. 66-74.
- [4] Wang Q., Tao S., Dubé C., Tury E., Ha, Y. J., Zhang S.,Khanizadeh S., Postharvest Changes in the Total Phenolic Content, Antioxidant Capacity and L-Phenylalanine Ammonia-Lyase Activity of Strawberries Inoculated with *Botrytis cinerea*. *Journal of Plant Studies*, 2012, 1(2), p. 11.

Sequestration of sludge C in soil as assessed by ¹³C abundance and ¹⁴C labelling

Stelmach W.^{1,2}, Shahbaz M.³, Bieganski A.¹, Kuzyakov Y.^{2,3}

¹ Institute of Agrophysics, Polish Academy of Science, Doświadczalna 4, 20-290 Lublin, Poland

² Dept. of Agricultural Soil Science, University of Göttingen, Büsgenweg 2, 37077 Göttingen, Germany

³ Dept. of Soil Science of Temperate Ecosystems, Büsgen-Institute, University of Göttingen, Büsgenweg 2, 37077 Göttingen, Germany

Corresponding author: Stelmach W., e-mail: w.stelmach@ipan.lublin.pl

Keywords: post-fermentation sludge, soil respiration, CO₂ efflux, Fe₂O₃, δ¹³C values, soil organic carbon, stabilization

Abstract

Stabilization of soil organic carbon (SOC) is important for natural ecosystems to sequester C and reduce greenhouse gas emissions. Biogeochemical processes closely coupling organic C with sesquioxides play an important role in stabilizing and destabilizing SOC. Iron oxide (Fe₂O₃) is an important regulator of SOC stability [1, 2]. It remains unclear, however, how organic fertilizers can be stabilized by Fe oxides to increase C sequestration in soil. The main aim of this study was to determine the effects of Fe₂O₃ on the sequestration of post-fermentation sludge in soil by tracing its decomposition and release of CO₂. The stability of sequestered sludge C in soil was assessed by adding glucose, to stimulate microbial activities.

Sludge was added at rates of 348 μg C g⁻¹ (equivalent to 200 kg N ha⁻¹). ¹⁴C-labeled glucose (15 μg C g⁻¹ ~ 10% of soil microbial C) was added 30 days later, after initial stabilization of sludge. Two isotopic approaches were used to partition the CO₂ efflux from SOC (δ¹³C = 28.8‰), sludge (δ¹³C = 16.8‰) and glucose (¹⁴C). This allowed quantification of the changes in SOC turnover after the addition of post-fermentation sludge, and its dependence on sorption on Fe₂O₃. Using natural abundance of the ¹³C isotope in the soil (which originated under C₃ vegetation) and in the post-fermentation sludge (produced from maize residues), we traced the CO₂ fluxes arising from both C sources [3].

Addition of the post-fermentation sludge to the soil increased CO₂ production 5 fold. Sorption of sludge on Fe₂O₃ halved the CO₂ efflux over 60 days. The input of glucose to partially decomposed and sorbed sludge increased its decomposition, as assessed by the increased CO₂ efflux with C₄ signature. Furthermore, the δ¹³C revealed that glucose strongly accelerated sludge decomposition even in Fe₂O₃ amended sludge, and so decreased C sequestration in soils.

We conclude that sorption of sludge and its stabilization on Fe₂O₃ can contribute to C sequestration in soil, but this C is not very stable under increasing microbial activities. These results have important implications for biogeochemical cycles and C stabilization. Such results were only possible to obtain by combining two isotopic approaches: ¹³C natural abundance and ¹⁴C labelling.

Acknowledgement

We thank the Catholic Academic Exchange Service (KAAD) and German Academic Exchange Service (DAAD) for the scholarship award for Wioleta Stelmach and Muhammad Shahbaz, respectively.

References

- [1] Kaiser K., Guggenberger G. The role of DOM sorption to mineral surfaces in the preservation of organic matter in soils. *Organic Geochemistry*, 2000, 31, pp. 711–725.
- [2] Guggenberger G., Kaiser K. Dissolved organic matter in soil: challenging the paradigm of sorptive preservation. *Geoderma*, 2003, 113, pp. 293–310.
- [3] Kuzyakov Y. Sources of CO₂ efflux from soil and review of partitioning methods. *Soil Biology & Biochemistry*, 2006, 38, pp. 425–448.

Modelling of Solar Air Heater Integrated with Dryer Chamber

Al-Neama M. A. and Farkas I.

Department of Physics and Process Control, Szent István University, Páter K. u. 1., Gödöllő, H-2100 Hungary

Corresponding author: Al-Neama M. A., e-mail: iqmay80@gmail.com

Keywords: air collector, modelling, solar energy, efficiency.

Abstract

In the recent period, the solar technologies and its applications becomes more and more important and efficient solution for many energy problems around the world. With using this form of renewable energy, our environment will be cleaner and our heat applications less expensive.

This study was carried out in a field solar energy at the Department of Physics and Process Control, Szent István University, Gödöllő, Hungary. The test rig consists from many parts as it is shown in Fig. 1. The flat plate solar collector has the size of 2 m x 0.5 m x 0.2 m. The solar collector with about 1 m² absorber plate area integrated to the dryer chamber to heat



Fig. 2 The scheme of the solar dryer

air flow that will enter the chamber. It has a transparent glass cover fixed on the top edges of the collector box and thermal insulation at the bottom base side of the metal box. For the better energy collection a black absorber plate was put on the half height of the collector body box. The solar collector in this work is oriented facing south line and tilted at 45° to the horizontal according to the solar chart for Budapest region (Budapest 47.5° N, 19.05° E). To get more absorption of solar radiation and radiation reflection reduction, absorber plate painted with matt black colour.

Effects of natural convection will be improved by adding a chimney in which exiting air is heated even more and enhance the buoyant flow of air. This will have a vital role to the overall design of solar dryers. Some study showed that the installation of three small fans and a photovoltaic cell is equivalent to the effect

of a 12 m chimney. Also a photovoltaic module with the maximum electrical power of 2x20 W and an electrical fan for good forced air circulation integrated with the system.

To simplify the model of solar collector, there are many considerations has been taken before simulation, as following:

1. Solar collector performance is steady state.
2. There is one-dimensional heat flow through back insulation.
3. Wind speed is approximately constant.
4. Air flow through the system is assumed homogeneous.
5. Air channel is assumed to be with no leakages.
6. Dust and dirt effects on the collector are neglected.

The energy balance on the solar collector totally is obtained by equating the total radiation gained from the sun rays (I) through the glass cover with transmittance (τ) to the total heat loosed from the absorber plate with area (A_c) of the solar collector. In the direction of air stream, the inlet ambient air to the collector carried sensible heat energy also depend on its mass mo and temperature $T_{c,i}$. The same for the outlet air, it will catch the heat from stored absorber plate energy by convection, then it will leave the solar collector with the same mass flow rate and new temperature equal to $T_{c,o}$. Then by considering the heat energy content for inlet and outlet air, the final energy balance for the air solar collector system will be:

$$\text{Useful heat} = (\alpha\tau) I A_c - \text{heat losses} + \text{inlet air heat content} - \text{outlet air heat content.}$$

Mathematically:

$$M C_p \frac{dT_{c,o}}{dt} = (\alpha\tau) I A_c - U A_c (T_c - T_\infty) + m^o C_p T_{c,i} - m^o C_p T_{c,o}$$

where M is the mass of air inside collector duct in (kg), T_∞ is the temperature of ambient air in (K), T_c is the average temperature of the absorber plate in (K), C_p is an air specific heat at constant pressure in (J/kg.K), $(\alpha\tau)$ is called transmittance-absorptance product for glazed collector, and it was for black colour absorber plate about 0.87, and U represents to the total energy losses from the flat plate solar collector; top, back (bottom) and side edges heat losses. For the last relation, a MATLAB simulation program has been developed to estimate the performance of air solar collector.

Acknowledgement

This paper was supported by the Stipendium Hungaricum Programme and the Mechanical Engineering Doctoral School at the Szent István University, Gödöllő, Hungary.

References

- [1] Al-Neama M.A., Farkas I.: Study of a solar energy drying system performance, Proceedings of the 5th European Drying Conference (EuroDrying'2015), Budapest, Hungary, October 21-23, 2015, pp. 22-27.
- [2] Al-Neama M.A., Farkas I., Performance enhancement of solar air collectors, Book of Abstracts, 14th International Workshop for Young Scientists (BioPhys Spring 2015), Gödöllő, Hungary, May 27-29, 2015, pp. 40-41.
- [3] Anderson T., Duke M., Carson J., Performance of colored solar collectors, The first international conference on applied energy, January 2009, Hong Kong.
- [4] Duffie J., Beckman W., Solar Engineering of Thermal Processes, Fourth edition, John Wiley & Sons, New Jersey, USA, 2013.
- [5] Kalogirou S.A., Solar energy engineering: process and systems, First edition, Elsevier's science and technology department in Oxford, England, 2009.

Current Status of the use of Solar Thermal Energy

Farkas I.

Department of Physics and Process Control, Szent István University,
Pater K. u.1., H-2100 Gödöllő, Hungary

Corresponding author: Farkas I., e-mail: farkas.istvan@gek.szie.hu

Keywords: cooling, concentrated solar power, heating, domestic hot water, passive solar

Abstract

The paper is going to deal with the overview of the worldwide position of the solar energy applications. Beside the technological issues the environmental questions will also be discussed.

The worldwide situation is analysed based on the recent development shown intensively at the Solar World Congress organized by the International Solar Energy Society at Daegu, Korea in 2015. Additionally, the most recently published books in this topic served also a basic source to the overview statements.

The main thematic questions are as follows:

1. Solar buildings and architecture
2. Resource assessment and energy meteorology
3. Renewable electricity technologies: PV
4. Renewable electricity technologies: CSP, biomass, geothermal, wind, hydro, ocean, and other
5. Solar heating and cooling
6. Solar energy and society
7. Energy storage
8. Renewable energy grid integration and distribution
9. Off-grid and rural energy access
10. Clean transportation technologies and strategies

Concerning to the future vision several recently published books are available which are listed in the reference list.

By the end of 2013 in the share of the total installed capacity in operation (including the glazed and unglazed water and air collectors is shown in Fig 2.

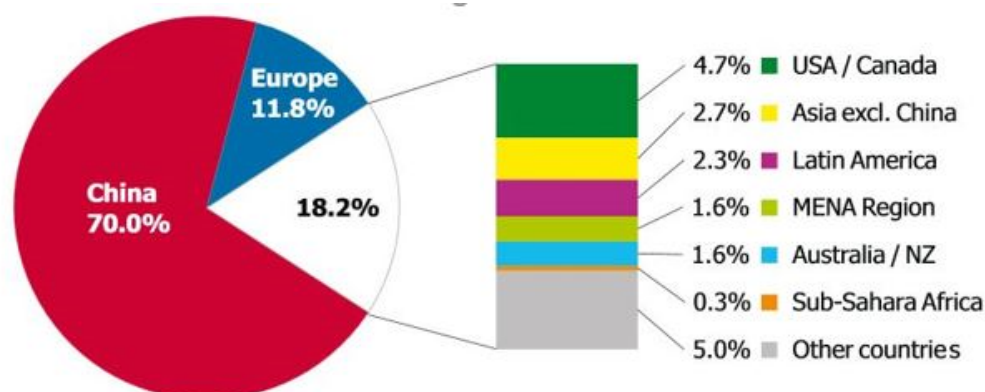


Fig. 1 Share of the solar thermal capacity by the end of 2013

Fig. 2 shows the global solar thermal capacity for the period of 2000-2014 justifying the importance of the solar heat (Mauthner, F., Weiss, W. and Spök-Dür, M., 2015).

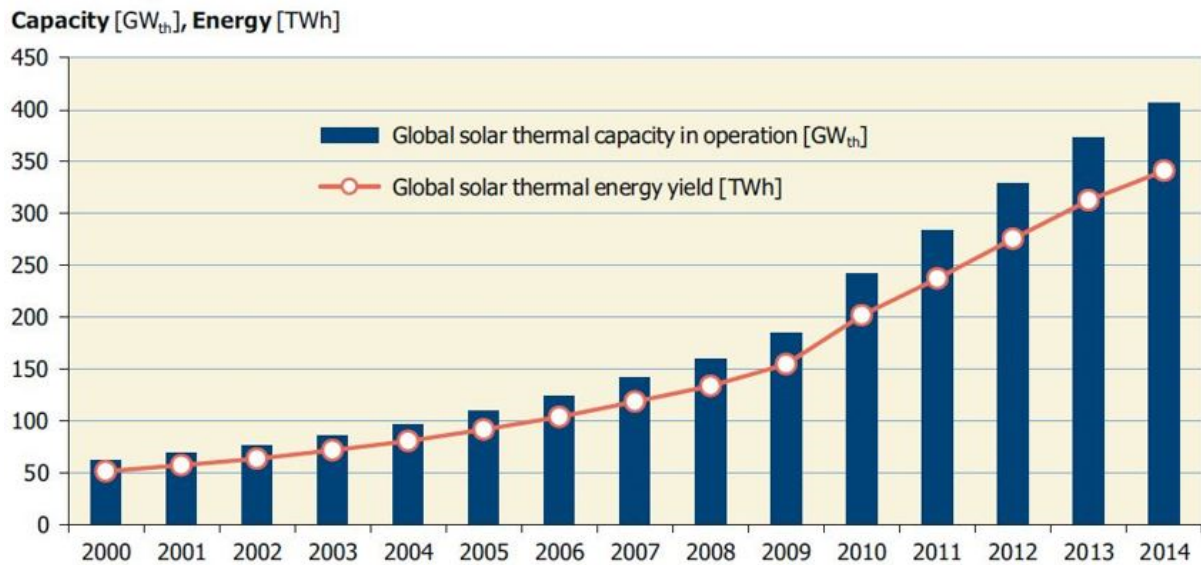


Fig. 2 Global solar thermal capacity and annual energy yields 2000-2014

The main issues of the use of solar thermal energy in Europe can be summarized along with the statements as:

- mainly solar domestic hot water systems are in use,
- growing share of combined systems,
- growing number of collective (large) systems,
- plastic absorber for swimming pool collectors,
- several solar district heating systems,
- pilot plants for process heat and for solar thermal assisted cooling systems.

Acknowledgement

The work was supported by the Mechanical Engineering Doctoral School, Szent Istvan University, Gödöllő, Hungary.

References

- [1] Mauthner, F., Weiss, W. and Spök-Dür, M. (2015), Solar heat worldwide, Markets and contribution to the energy supply - 2013, SHC - Solar Heating and Cooling Programme, International Energy Agency
- [2] Renewables 2015 - Global Status Report, REN 21, Renewable Energy Policy Network for the 21th Century
- [3] Rethinking energy (2015), Renewable energy and climate change, IRENA
- [4] SDH - Solar district heating, 2012, Market for solar district heating, CIT Energy Management AB
- [5] Strategic research priorities for solar thermal technology, 2013, RHC – Renewable Heating and Cooling European Technology Platform
- [6] Weiss W., 2013, Current status of solar thermal application worldwide, AEE, Institute for Sustainable Technologies, Gleisdorf, Austria

Symmetry Analysis of Collective Elementary Excitations of Chain-type Organic Molecules, relevant for Solar Cells

Mészáros Cs.¹, Nikolényi I.¹, Bálint Á.²

¹ Department of Physics and Process Control, Institute for Environmental Engineering Systems, Szent István University, Páter K.u.1., H-2103 Gödöllő, Hungary

² Institute of Environmental Engineering, Óbuda University, Sándor Rejtő Faculty of Light Industry and Environmental Engineering, Doberdó u. 6, Budapest, Hungary, H-1034e

Corresponding author: Mészáros Cs., e-mail: Meszaros.Csaba@gek.szie.hu

Keywords: chain-type molecules, collective elementary excitations, solar energy

Abstract

It is well-known nowadays, that the detailed experimental and theoretical investigation of basic structural and physical properties of different types of carbon nano-tubes plays a role of continuously increasing importance in the whole condensed matter physics [1]. The detailed symmetry analysis of all these aspects represents a crucial part of investigation of all the relevant problems being investigated. One of the most successful mathematical techniques from this point of view is related to detailed application of the abstract-, and representation theory of quasi-one-dimensional (Q1D) systems, also known under the name of line groups [2], and which is a genuine mathematical basis for structural investigation of polymers by diffraction methods for decades [3]. Among the newest methods of investigations of such types of condensed matter systems, research activities connected to possible applications in solar cells became also very significant, e.g. [4], despite of the fact, that in the most detailed quantum-statistical descriptions of collective elementary excitations relevant for light absorbing organic materials the selection rules based on the line group theory have not been applied [5], but which may be of importance in the case of modelling of the exciton-type collective modes, too. In the present work we will demonstrate in detail some further possible and very promising application of the same mathematical technique relevant for chain-type molecular systems, which may contribute to understanding and increase of the energy transformation efficiency in solar energetics, too.

In order to contribute to a detailed future research programmes in the above given sense, we will present here some basic relations about quantum mechanical selection rules, on the base of the representation theory of line groups. It is a crucial mathematical feature of this formalism, that the point groups of the molecular motifs (which are the monomers in the case of stereoregular polymers) are not independent of the possible translations along the main axis of the system. The screw-axes of rational order are also allowed in this theory, which is not characteristic for the mathematical formalism of classical crystallography.

Then, according to the definition, the complete set of symmetry transformations leaving invariant a Q1D system belongs to one of the (discrete) infinitely many line groups gathered into 13 families [2]. The irreducible representation $D^{(\mu)}(L)$ of a full line group L can be obtained from the irreducible representation of symmetry groups (i.e. point groups) of the motifs $D^{(\nu)}(P)$ by use of the induction technique elaborated in the theory of group representations and widely applied in solid state physics [6] and is usually denoted by $D^{(\mu)}(L) = D^{(\nu)}(P) \uparrow L$. On the base of this formalism, the formulae necessary for quantum-mechanical selection rules between an initial („i“) and final („f“) state in chain-type systems are („k“ denotes the absolute value of a wave vector, „j“ is an integer number, and „a“ is the length (i.e. generating element) of the possible allowed translations along the main axis of a Q1D system being investigated):

$$k_f - k_i = k + 2\pi j/a.$$

Furthermore, it is a unique feature of the representation theory of line groups, that analogous relations expressing conservation of quasi-angular momenta during propagation of collective excitations along the main axis of the actual chain-type system must also be taken into account, i.e.:

$$m_f - m_i = m + zq,$$

where „m“ denotes the value of the momentum, „z“ is an integer number, while „q“ is the order of a simple cyclic rotation group, also characterizing allowed integer translations along the main axis of the system. In the present study, all these relations will be applied in detail and incorporated into correlation functions necessary for comparison of experimentally measured-, and theoretically derived light scattering intensity curves.

Finally, the following remark of general character must also be made. Although some applications of the projective representations of crystallographic point groups in solid state physics are known for decades, they are completely absent even from the most complete works about applications of line groups in various types of structural investigations of condensed matter systems. In order to overcome this problem, we applied our own earlier result [7] about generalized-type description of structure factors (realized by a simple, but completely novel-type use of projective representations in the case of incommensurately modulated crystals) to extend [8] the existing Fourier-analysis formalism relevant for interpretation of the diffuse X-ray scattering intensity curves.

References

- [1] Barros, E. B., Jorio, A., Samsonidze, G.G., Capaz, R.B., Souza Filho, A.G., Mendes Filho, J., Dresselhaus, G., Dresselhaus, M.S., Review on the symmetry-related properties of carbon nanotubes. *Physics Reports*, 2006, 431,6, pp. 261-302.
- [2] Damnjanović, M., Milošević, I., 2010, *Line Groups in Physics (Theory and Applications to Nanotubes and Polymers)* Springer-Verlag, Berlin-Heidelberg
- [3] Vainshtein, B.K., 1966, *Diffraction of X-Rays by Chain Molecules*, Elsevier Publ. Co., Amsterdam
- [4] Li, T.S., S C Chang, S.C., Lien, J.Y., Lin, M.F., 2008, Electronic properties of nanotube-ribbon hybrid systems, *Nanotechnology* **19** 105703
- [5] Agranovich, V., *Excitations in Organic Solids*, 2009, International Series of Monographs on Physics, University Press, Oxford
- [6] Streitwolf, H.W., 1967, *Gruppentheorie in der Festkörperphysik*, Akademische Verlagsgesellschaft: Geest & Portig, Leipzig,
- [7] Kirschner, I., Mészáros, Cs., Laiho, R., 1998, Line group theory of commensurate and incommensurate modulations. *European Journal of Physics B* 2, 2, pp. 191–196.
- [8] Bálint, Á., Nikolényi, I., Mészáros, Cs., 2015, General symmetry properties of incommensurately modulated crystals described by projective representations of line groups, *Journal of Universal Science Online*, 2,2, pp. 10-17.

Biophysical experiments on human senses

I. Seres

Department of Physics and Process Control, Szent István University, Páter K. u. 1., Gödöllő,
H-2103, Hungary

Corresponding author: István Seres, e-mail: Seres.Istvan@gek.szie.hu

Keywords: biophysics, senses, experiments

Abstract

The experience of the BPS conferences from the last few years prove, that beside the numerous theoretical presentations introducing research results, more practical topics made interesting by experiments can be useful for the participants, as well. During the last few years we introduced a few special topics through experiments, connected to the biophysics, as non-Newtonian liquids, or material behavior under special conditions (very low temperature, very low pressure). The positive feedback from these meetings encouraged us to continue carrying out experiments to demonstrate the importance of the practice and to popularize the Physics.

One big advantage of this conference series, that PhD students and scientists from different fields of the science are joining (chemist, biologist, physicist, engineers), so it is a nice possibility to widen the breath of view of the participants. The aim of this presentation is to show how a physics lecturer thinks about the working of the human senses, and with what sort of experiments can be this demonstrated.

With our data loggers – however sometimes they are a bit more accurate- generally we want to simulate the human senses (vision, hearing, touch, taste, smell), but generally our technical devices are much less adaptive and sensitive than the sensors developed by the evolution, our senses. In the presentation the extremely wide range of our senses is demonstrated, by comparing them with some technical devices.

After discussing some general properties e.g. the biophysical Weber-Fechner law, which concludes, that our senses convert the physical signal to sense through a logarithmic function – that is the reason why our sound level meters converting the intensity to decibel by a logarithmic function of $dB = 10 \cdot \lg \frac{I}{I_0}$.

When studying the different senses alone, some experiments can be done for each, to find the general rules of operations. For example it is not so widely known, that our senses can work much better in relative scale than in absolute one. Some experiments are planned to demonstrate this for example for the heat sensing and the hearing. For the first, if someone holds her/his one hand in cold water and the other one in warm water for a little while, and after that each of his hands are taken to the same (medium temperature) water, with the two hands she/he feels different temperatures. Similarly a few people can recognize a small difference between two generated sounds (with a few Hz difference between them), but if the two are played together, then the difference seems to be evidence.

Because of its highest importance, special attention is planned to be taken to the vision. There are some really funny examples how eyes can be made fool by the colour sensing. With the help of the RGB colour coordinates of regions in specially prepared pictures it can be proved, that colours, identified by our eyes as obviously different, are identical. The reason for it, that our eyes do not sense the colour of the objects alone, but as a comparison to the surroundings.

Another important field for the experiments of the 3D vision of the eye. The principle of the spatial vision is, that our two eyes see different pictures from the surrounding objects because of the given distance between our eyes. Some technical methods will be presented, what sort of technical solutions were tried to have the same feeling in the different 3D technologies. Some of them need technical supplements, as e.g. polar filters for the 3D movies, but there are

technics without technical devices, as e.g. the stereograms. As not everybody can see stereograms, a short course is planned on how to see them.

Another interesting question is, that if somebody do not have two eyes, how her/his 3D imaging is working. To demonstrate this, a model of the so called Ames room will be introduced. In this case our vision recognize things, which are obviously against to our knowledge, although they seems to be true.

An approximate list about the experiments planned to show:

- the relative sense of temperature
- sound beat (acoustics) – the strange effect of two sounds with small frequency difference
- ultrasound – the limits of the human hearing
- a simple, but effective method for sound encryption
- How we recognize the different instruments?
- experiments with colours
- 3D vision
- Ames room model
- optical illusions – to see the impossible
- How the RGB works
- detect the insensible – measuring radioactive background

Acknowledgement

This paper was supported by the Mechanical Engineering PhD School, Szent István University, Gödöllő, Hungary.

References

- [1] Jay Nadeau (2013): Introduction to Experimental Biophysics: Biological Methods for Physical Scientists, CRC Press, Taylor and Francis Group
- [2] V. Pattabhi, N. Gautham (2002): Biophysics, Kluwer Academic Publishers, New Delhi

Refinement of temperature data in soil column experiments

Tóth J.¹, Mészáros Cs.¹, Bálint Á.²

¹Department of Physics and Process Control, Faculty of Mechanical Engineering, Szent István University, Páter K. u. 1., Gödöllő, H-2103, Hungary

²Institute of Environmental Engineering, Óbuda University, Doberdó út 6., Budapest, H-1034, Hungary

Corresponding author: Tóth J., e-mail: toth-janos@outlook.com

Keywords: MATLAB, data analysis

Abstract

The heat transport in the soil and the heat transport between the soil and the air is very important process from agricultural point of view. This is a complex process, so the relevant mathematical model can be verified by adequate measurement methods. After the correction of the data the evaluation process can be done [1].

The measurements were realized in Potsdam, Germany in September, 2015. These measurements focused on the temperature and the moisture level of the soil. The data of the moisture content were detected by tensiometers. The data concerning temperature were captured by thermal sensors, connected to an Almemo data collecting device, and by an infrared camera.

The first task of the evaluation was to repair the corrupted files, because there was some communication problem between the Almemo device and the PC. For this, a program was written by us, that could do this kind of reparation and it could produce an output file for MATLAB, that we used to the further evaluation.

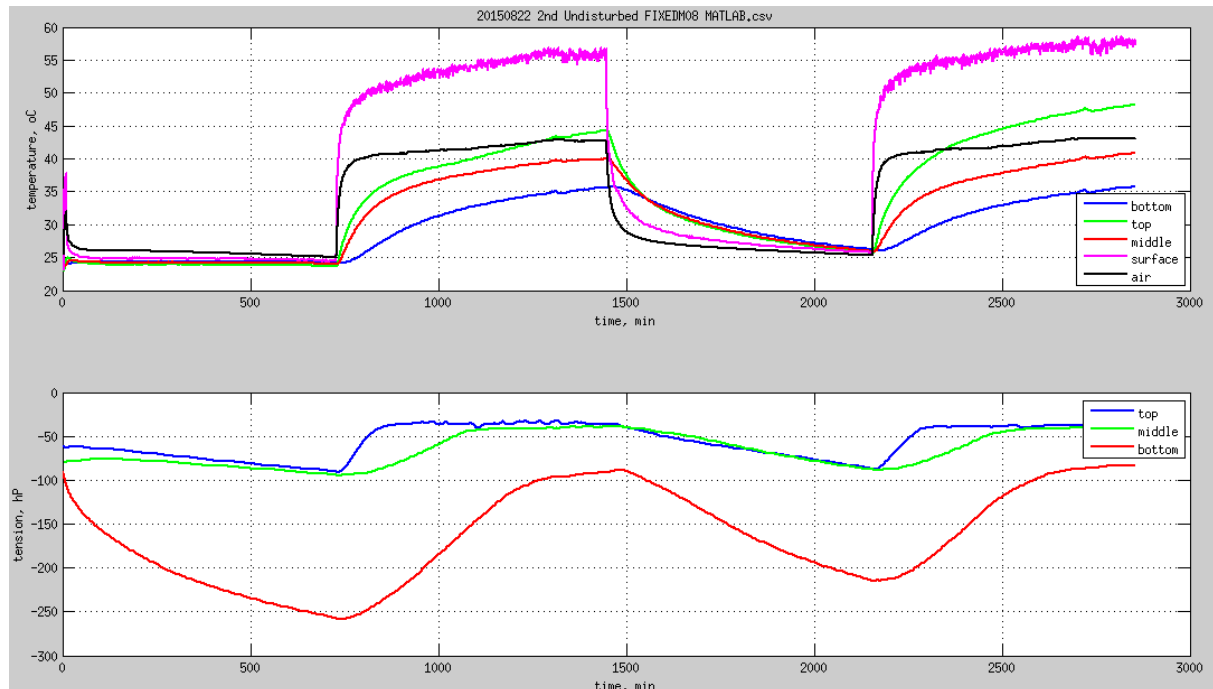


Fig. 1 Soil temperature and tension data captured by the Almemo device

The next step was to read the temperature data saved by the camera, and convert it to a MATLAB-compatible format.

The infrared camera was also not calibrated, so it has to be corrected its data based on the data saved by the Almemo device. For this purpose, an objective function was implemented in MATLAB system and did a minimum search on it. After that the calculated coefficients were used what was the parameters of the objective function, to calibrate the remaining results.

The results of the measurements collected by the camera had to be corrected because there were some unrealistic sections on the temperature function, caused by the lack of the calibration.

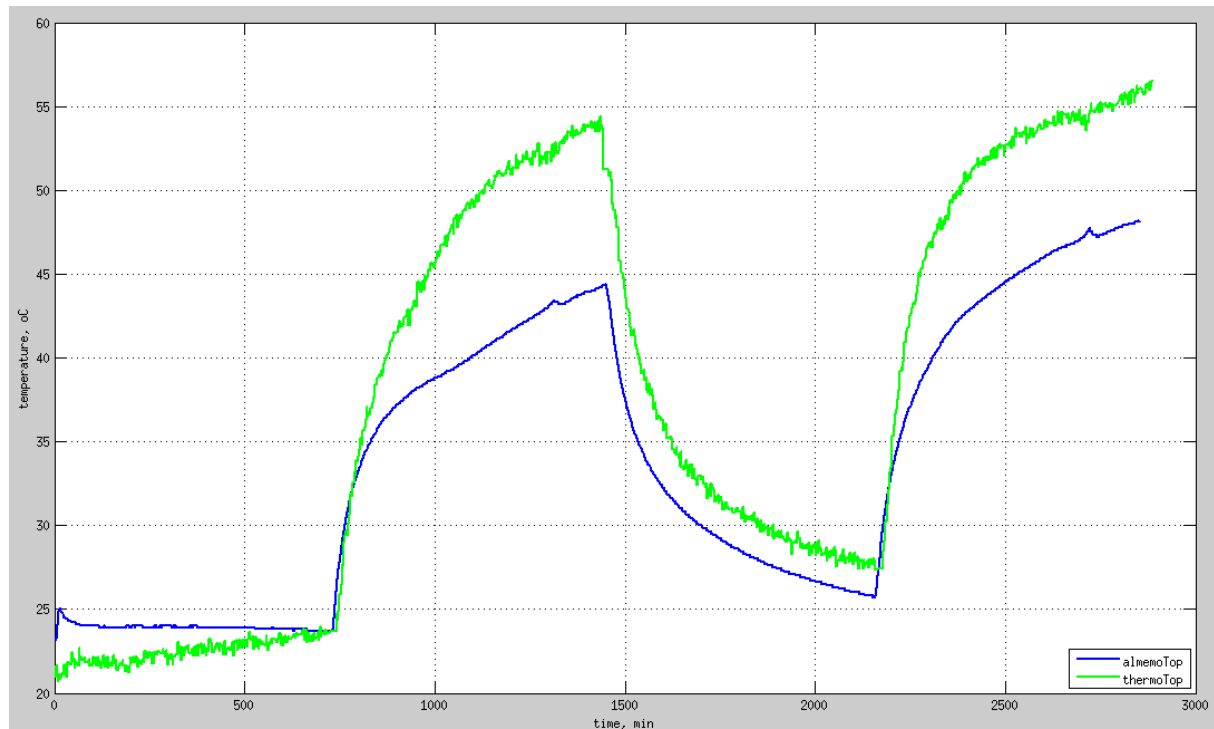


Fig. 2 Corrected temperature data of the infrared camera (blue), reference temperature data from the Almemo device (green)

The further task will be to continue the evaluation by performing additional analysis on the data collected.

Acknowledgement

This work was supported by the MÖB/DAAD Project No. 55731.

References

- [1] Kosztlányi R., Bálint Á., Gottschalk K., Mellmann J., Kozma I., Tóth J., Mészáros Cs.: Analysis of heat transport in soil column measurements simulating sun cycle, Szent István University Faculty of Mechanical Engineering, Mechanical Engineering Letters, Gödöllő, Hungary, 2015, Vol. 13, pp. 115-121., HU ISSN 2060-3789

Physical properties of birch sap

Víg P.

Department of Physics and Process Control, Szent István University, Páter K. u. 1., Gödöllő, H-2103, Hungary

Corresponding author: Víg P., e-mail: Vig.Piroska@gek.szie.hu

Keywords: birch sap, surface tension, viscosity, refractive index

Abstract

Today, in the civilized regions the role of the healthy lifestyle is increasing, and the quality food usage is its important part. The crops nowadays have only the fraction of the inner worth, than they had 50 years ago [1], which confirms the consumption of extra vitamin and mineral at the end of winter and spring time. But it is important to know, that the wild growing foods - which are not treated with chemicals and do not use on them yield enhancement - inner worth is remained relatively high [1], so their consumption is an important natural vitamin and mineral source.

For these sources offered by the nature is a good example the birch sap, the juice of the birch tree. Based on studies [2], its compositions are very important. It externally can be used for care of skin and hair, consumed internally it strengthens the immune system, cleans the blood and lymphatic system, it have detoxification effect and support the urinary and digestive systems [3].

Birch sap can be obtained in spring from the beginning of the circulation and appearance of the small leaves, up to 3-4 week time period with tapping of the tree. With help the recess of the trunk or break small branch, appears liquid drops. They have similar texture than the fresh water with sweet taste and aroma of birch tree. This collected liquid can be consumed fresh or fermented beverages, too [4]. Already since the 13th century there are written records about its consumption and medicinal effect, mainly regions of Russia, Ukraine, Finland, Estonia, Latvia, Sweden, England and Scotland, Czech Republic, Poland, Hungary and Romania.

The aim of this work is to examine the physical properties of the birch sap. The examined sap made from the birch trees which is located in our garden, in Gödöllő, Hungary.



Fig. 1 Birch sap gathering

The evolution of surface tension, viscosity and refractive index are examined during the collection period. The tapping occurred by breaking small branches and with fixation a bottle around the broken surface (Fig. 1).

From the bottles the sap was collected twice a day, at 7 in the morning and evening, and the collected material was uploaded into a glass jar and these samples were stored until the measurement in the fridge.

The dependence the yield on rainfall and was investigated, and if there is difference between the physical properties of the night and day gathered sap.

I examined whether the expiry of the use-by date can lead to a change in the examined physical characteristics? Fresh birch sap is highly perishable; even if refrigerated, it is stable for only up to 2-5 days. I examined the physical characteristics evolution of the fresh birch sap function on storage time.

Shelf life can be prolonged by freezing or preservation techniques. Examples: filtered with a 0,22c μ net (shelf life: 3 weeks refrigerated), collected under anaerobic conditions (shelf life: 1 year ambient), heat pasteurized; pasteurization should be conducted under specific temperature levels and time spans (shelf life: 1 year ambient). Although level of Vitamin C is lower than fresh saps, all benefits are preserved. Frozen at -25 °C (shelflife: 2 years).

During the determination of refractive index Abbe refractometer, for viscosity measuring Höppler viscosimeter and during the surface tension determination stalagmometer was used (Fig. 2).



Fig. 2. The used equipments (refractometer, viscosimeter, stalagmometer)

The presentation details the measurements, summarizes the results from the measurement data and conclusions.

Acknowledgement

This paper was supported by the Mechanical Engineering PhD School, Szent István University, Gödöllő, Hungary.

References

- [1] Márai, G.: Analysis of the change of nutrient microelements and vitamin contents, http://www.biokontroll.hu/cms/images/stories/eloadasok/Bardocz-Pusztai_eloadasa_Eltero_gazdalkodasi_rendszerekbol_szarmazo_elelmiszerek.pdf, 2016.
- [2] Svanberg, Ingvar; et al. Uses of tree saps in northern and eastern parts of Europe. *Acta Societata Botanicorum Poloniae*, 2012, 81(4):343–357.
- [3] Tomoko, S. Birch sap: survey on traditional uses and their impacts on future uses. *Tree Sap, Proceedings of 3rd International Symposium on Sap Utilization (ISSU)*. Hokkaido University Press, 2005, 53–59.
- [4] Ahtonen, S; Kallio, H. Identification and seasonal variation of amino acids in birch sap used for syrup production. *Food Chemistry* 1989, 33 (2): 125–132.



Czech University of Life Sciences, Prague

Department of Physics

Kamýcká 129, 16521 Prague 6

Czech Republic

ISBN 978-83-89969-42-2